Clim. Past, 10, 1421–1439, 2014
www.clim-past.net/10/1421/2014/
doi:10.5194/cp-10-1421-2014

Climate of the Past
Open Access

Warming, euxinia and sea level rise during the Paleocene–Eocene Thermal Maximum on the Gulf Coastal Plain: implications for ocean oxygenation and nutrient cycling

A. Sluijs[1], L. van Roij[1], G. J. Harrington[2], S. Schouten[3,4], J. A. Sessa[5,6], L. J. LeVay[6,7], G.-J. Reichart[3,4], and C. P. Slomp[4]

[1]Marine Palynology and Paleoceanography, Department of Earth Sciences, Faculty of Geosciences, Utrecht University, Laboratory of Palaeobotany and Palynology, Budapestlaan 4, 3584CD, Utrecht, the Netherlands
[2]School of Geography, Earth and Environmental Sciences, Aston Webb Building, University of Birmingham, Birmingham, B15 2TT, UK
[3]NIOZ Royal Netherlands Institute for Sea Research, P.O. Box 59, 1790 AB, Den Burg, Texel, the Netherlands
[4]Department of Earth Sciences, Faculty of Geosciences, Utrecht University, Budapestlaan 4, 3584CD, Utrecht, the Netherlands
[5]Devision of Paleontology, American Museum of Natural History, Central Park West at 79th St., New York, NY 10024, USA
[6]Department of Geosciences, Pennsylvania State University, University Park, PA 16802, USA
[7]International Ocean Discovery Program and Department of Geology and Geophysics, Texas A&M University, College Station, Texas 77845, USA

Correspondence to: A. Sluijs (a.sluijs@uu.nl)

Received: 8 November 2013 – Published in Clim. Past Discuss.: 3 December 2013
Revised: 28 March 2014 – Accepted: 16 June 2014 – Published: 25 July 2014

Abstract. The Paleocene–Eocene Thermal Maximum (PETM, ∼56 Ma) was a ∼200 kyr episode of global warming, associated with massive injections of ^{13}C-depleted carbon into the ocean–atmosphere system. Although climate change during the PETM is relatively well constrained, effects on marine oxygen concentrations and nutrient cycling remain largely unclear. We identify the PETM in a sediment core from the US margin of the Gulf of Mexico. Biomarker-based paleotemperature proxies (methylation of branched tetraether–cyclization of branched tetraether (MBT–CBT) and TEX_{86}) indicate that continental air and sea surface temperatures warmed from 27–29 to ∼35 °C, although variations in the relative abundances of terrestrial and marine biomarkers may have influenced these estimates. Vegetation changes, as recorded from pollen assemblages, support this warming.

The PETM is bracketed by two unconformities. It overlies Paleocene silt- and mudstones and is rich in angular (thus in situ produced; autochthonous) glauconite grains, which indicate sedimentary condensation. A drop in the relative abundance of terrestrial organic matter and changes in the dinoflagellate cyst assemblages suggest that rising sea level shifted the deposition of terrigenous material landward. This is consistent with previous findings of eustatic sea level rise during the PETM. Regionally, the attribution of the glauconite-rich unit to the PETM implicates the dating of a primate fossil, argued to represent the oldest North American specimen on record.

The biomarker isorenieratene within the PETM indicates that euxinic photic zone conditions developed, likely seasonally, along the Gulf Coastal Plain. A global data compilation indicates that O_2 concentrations dropped in all ocean basins in response to warming, hydrological change, and carbon cycle feedbacks. This culminated in (seasonal) anoxia along many continental margins, analogous to modern trends. Seafloor deoxygenation and widespread (seasonal) anoxia likely caused phosphorus regeneration from suboxic and anoxic sediments. We argue that this fueled shelf eutrophication, as widely recorded from microfossil studies, increasing organic carbon burial along many continental

margins as a negative feedback to carbon input and global warming. If properly quantified with future work, the PETM offers the opportunity to assess the biogeochemical effects of enhanced phosphorus regeneration, as well as the timescales on which this feedback operates in view of modern and future ocean deoxygenation.

1 Introduction

The Paleocene–Eocene Thermal maximum (PETM; ∼ 56 Ma) is one of at least three geologically brief (< 200 kyr) global warming events, often referred to as "hyperthermals" (Thomas and Zachos, 2000), superimposed on a long-term late Paleocene–early Eocene warming trend (Zachos et al., 2008; Bijl et al., 2013; Frieling et al., 2014). The PETM is marked by a ∼ 2–7 ‰ negative carbon isotope excursion (CIE), recorded in marine and terrestrial sedimentary components, and carbonate dissolution in deep-sea sediment records (Sluijs et al., 2007a). These phenomena indicate a massive injection of ^{13}C-depleted carbon into the ocean–atmosphere system, but the mechanism for this release remains controversial (Dickens, 2011). Although coverage for low-latitude regions is limited, the available information suggests that the global average surface temperature warmed by 4–5 °C (Kennett and Stott, 1991; Zachos et al., 2003; Sluijs et al., 2006; Dunkley Jones et al., 2013). A rise in sea level has been recorded along several mid- to high-latitude continental margins (e.g., Speijer and Morsi, 2002; Harding et al., 2011), suggesting eustatic rise (Sluijs et al., 2008a).

The PETM is characterized by major biotic response, including global dominance of the dinoflagellate *Apectodinium* and the extinction of ∼ 50 % of the deep-sea benthic foraminifera species (Sluijs et al., 2007a). Moreover, the PETM is globally recognized as a major catalyst in mammal migration and evolution, including the first and widespread occurrence of primates (Bowen et al., 2002). The causes of biotic change, notably for the marine realm, remain largely uncertain (Gibbs et al., 2012). One of the proposed forcing mechanisms for marine biotic change has been deoxygenation (Thomas, 2007). This is because several studies have presented evidence of a decrease in water column oxygen content in deep, intermediate and shallow settings, although the full extent and consequences remain unclear (Speijer and Wagner, 2002; Sluijs et al., 2006; Chun et al., 2010; Dickson et al., 2012).

Previous work has attempted to locate the PETM in sediment sequences along the US Gulf Coastal Plain (GCP; Georgia to Texas; Fig. 1) (e.g., Harrington et al., 2004; Beard, 2008). Beard (2008) suggested that a channel sand deposit named the T4 sand at the Red Hot Truck Stop (RHTS) locality in Meridian, Mississippi, represents the early stages of the PETM, and attributed a subsequent hiatus to sea level fall during the PETM. A primate fossil found within this channel sand was therefore hypothesized to be the oldest North American primate on record, leading to revised migrational patterns of these early primates (Beard, 2008). Here, we present a multiproxy stratigraphic, paleoecologic, and paleoclimatologic study of late Paleocene and early Eocene sediments recovered in the Harrell Core, which was drilled by the Office of Geology of the Mississippi Department of Environmental Quality near Meridian, MS (NE, NW, NW, NW, Township 15N, Range 15E, Section 24, Lauderdale County; converted to latitude and longitude using www.earthpoint.us: 32°15′04″ N, 88°43′14″ W), and ∼ 9.7 km south-southwest of the Red Hot Truck Stop locality (Fig. 1). We analyzed physical sediment properties, organic matter (bulk and compound specific) carbon isotope ratios, palynology (dinoflagellate cysts, pollen, and spores),

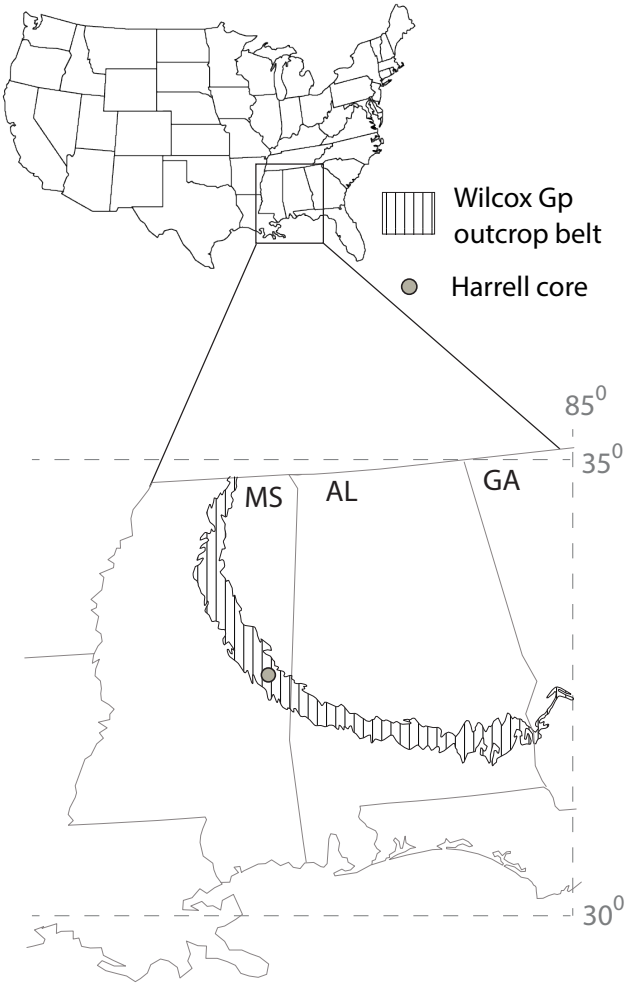

Figure 1. Location map of the Harrell Core in Meridian, Lauderdale Co., Mississippi, USA, and outcrop belt of the Wilcox Group, comprising the Paleocene and early Eocene Nanafalia, Tuscahoma and Hatchetigbee formations along the eastern Gulf of Mexico. Map was modified from Schruben et al. (1998).

and calcareous nannofossils to document climate change and ocean oxygenation through this interval. The first identification of the PETM within the GCP and documentation of sea surface and continental warming has regional implications for stratigraphy and primate migration patterns. Moreover, these new data, combined with an extensive data compilation, suggest that ocean deoxygenation played a major role in nutrient cycling, biotic changes, and carbon cycle evolution during the PETM.

2 Regional stratigraphy

Upper Paleocene and lower Eocene deposits along the GCP are primarily fine sands, silts, and siliciclastic muds, with intermittent lignites. Thin, mixed carbonate–siliciclastic beds occur throughout this interval; carbonate deposition was most prominent in what is now Alabama (Dockery, 1980; Mancini, 1981; Mancini and Oliver, 1981; Gibson et al., 1982; Mancini and Tew, 1991, 1993; Gibson and Bybell, 1994; Mancini and Tew, 1995; Sessa et al., 2012b). This indicates a "proto" Mississippi River embayment with large deltaic systems spread across the eastern GCP (Mississippi through Georgia; Fig. 2) at that time; the Laramide Rocky Mountains provided the source of siliciclastic supply (Galloway et al., 2000). The Tuscahoma Formation (Fm), the uppermost part of the middle Wilcox Group, underlies the Bashi member of the Hatchetigbee Fm, which is the basal unit of the upper Wilcox Group (e.g., Gibson and Bybell, 1994) (Fig. 2). The hierarchical status of the Bashi sediments has not been consistent amongst authors (e.g., Gibson and Bybell, 1981, 1994; Gibson, 1982; Harrington and Jaramillo, 2007; Beard and Dawson, 2009) because of controversy regarding whether it is a formation or a member (Gibson, 1982; Dockery et al., 1984). We follow the taxonomy of Gibson and Bybell (1994), who consider the Bashi to represent a member of the Hatchetigbee Fm.

The stratigraphy and depositional environments of the Tuscahoma and Hatchetigbee formations from the eastern GCP have been the subject of multidisciplinary studies of pollen (Tschudy, 1973; Frederiksen, 1998; Harrington, 2001, 2003; Harrington and Jaramillo, 2007), plants (Danehy et al., 2007), mammals (Beard and Dawson, 2001; Beard, 2008), dinoflagellate cysts (Edwards and Guex, 1996), planktonic foraminifera (Mancini, 1981; Mancini and Oliver, 1981), calcareous nannoplankton (Gibson et al., 1982; Siesser, 1983; Gibson and Bybell, 1994), mollusks (Dockery, 1980, 1998; Sessa et al., 2012a), magnetostratigraphy (Rhodes et al., 1999), and sequence stratigraphy (Baum and Vail, 1988; Mancini and Tew, 1993, 1995) (Fig. 2).

The Tuscahoma Fm was found to be within Magnetochron C24r by Rhodes et al. (1999). Within the middle Tuscahoma Fm is the Bells Landing Marl, a thin (maximum of 3 m thickness) marine incursion formed during a transgressive systems tract (Baum and Vail, 1988; Mancini and Tew, 1991, 1993, 1995). The occurrence of the planktic foraminifers *Morozovella subbotinae* and *M. velascoensis* (Mancini and Oliver, 1981) restrict the age of the Bells Landing Marl to the time interval spanning the latest Paleocene (zone P5 of Wade et al., 2011) through the earliest Eocene (zone E2). The occurrence of *Pseudohastigerina wilcoxensis* would suggest an earliest Eocene age (Wade et al., 2011). However, diachronicity between the GCP and Africa, where the range of this species was calibrated, cannot be excluded. Mancini and Oliver (1981) note that *P. wilcoxensis* likely evolved from *Planorotalites chapmani* during the late Paleocene, partially based on the "somewhat atypical" specimens of *P. wilcoxensis* found in lower Tuscahoma marls. If *P. wilcoxensis* evolved in the study region, it may not be surprising if its first occurrence was earlier here than in Africa. Indeed, its first occurrence was previously reported to be diachronous with latitude (Pardo et al., 1997). Moreover, Gibson et al. (1982) and Siesser (1983) determined that the Bells Landing Marl represents the late Paleocene (calcareous nannofossil zone NP9). This is based on the occurrence of *Discoaster multiratiatus* and the combined absence of *Tribrachiatus* spp., and *Rhomboaster* spp., which excludes an age younger than NP9. Both *Tribrachiatus* and *Rhomboaster* are heavily calcified genera that are resistant to dissolution, making it unlikely that preservation accounts for their absence. To our knowledge, there is no report of a nannofossil species in the Bells Landing Marl that would suggest an age younger than late Paleocene (zone NP9).

Above the Bells Landing Marl, the Tuscahoma Fm, particularly within the studied region (Fig. 1), consists of micaceous and glauconitic sands and silts with intermittent lignites representing estuarine and lagoonal environments (Ingram, 1991), with little to no carbonate and no calcareous microfossils (Gibson and Bybell, 1994). The uppermost beds of the Tuscahoma Fm yield brackish to freshwater palynomorphs, notably pollens and spores of late Paleocene affinities (e.g., Frederiksen et al., 1982; Frederiksen, 1998; Harrington, 2003). Collectively, the available information indicates a late Paleocene age of the Tuscahoma Fm (e.g., Gibson and Bybell, 1994; Harrington, 2003; Beard, 2008).

Throughout the eastern GCP, the Tuscahoma Fm is unconformably overlain by the Bashi Member (Mb), which includes a transgressive lag composed of glauconitic and calcareous marl and sand, representing an inner shelf environment (Dockery, 1980, 1998; Gibson, 1982; Mancini, 1984; Siesser, 1983; Ingram, 1991; Mancini and Tew, 1991, 1995; Sessa et al., 2012b). This layer contains abundant mollusk and vertebrate fossils and often is lithified into large (1–2 m long) concretions, making it recognizable in both outcrop and core. Sessa et al. (2012b) suggested that the Meridian, MS outcrops of this marine incursion were deposited very near to the paleoshoreline because of their relatively coarser-grained sands, trough cross-bedding, and *Ophiomorpha* burrows (see also Dockery, 1980; Ingram, 1991; Gibson and Bybell, 1994).

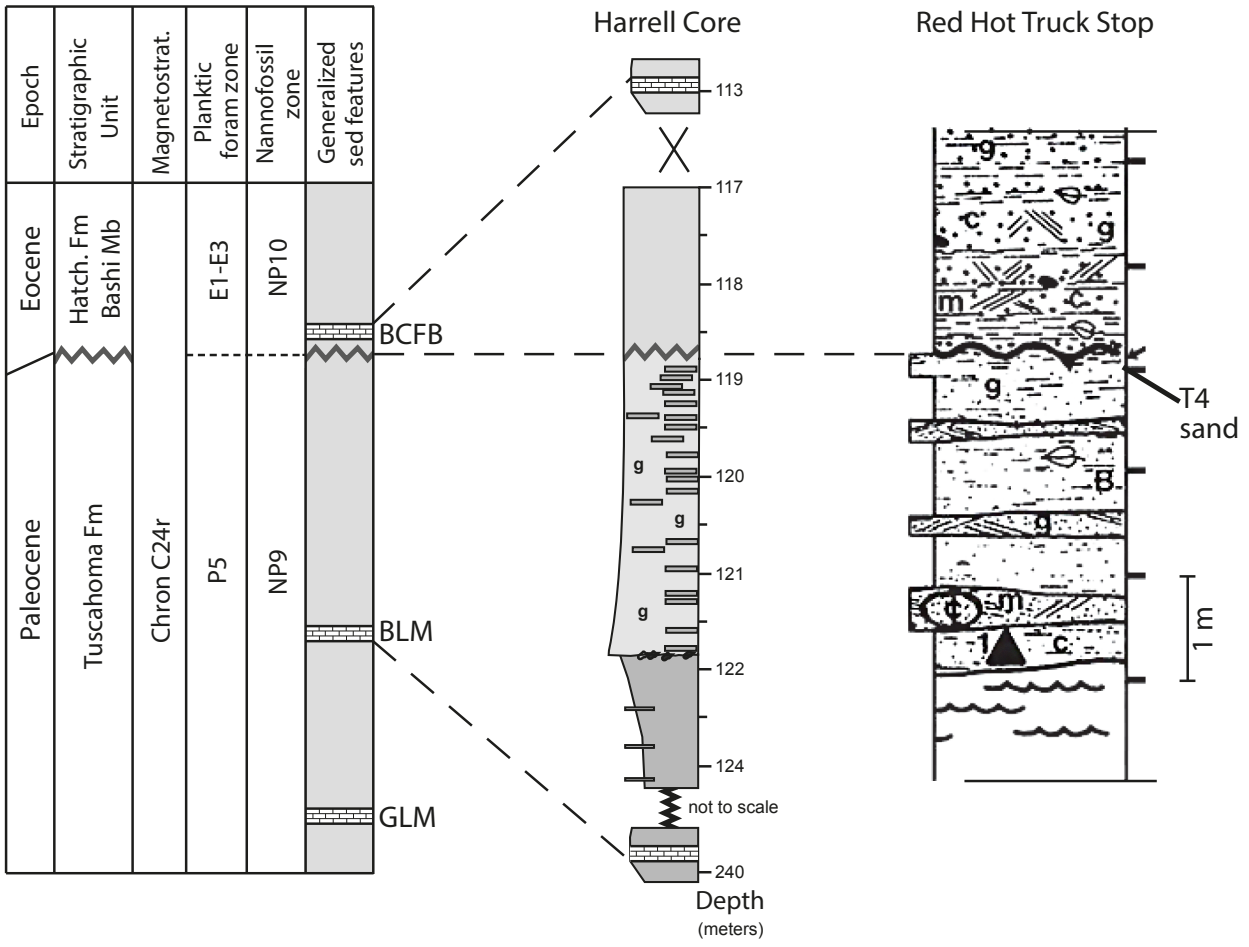

Figure 2. Schematic stratigraphy of upper Paleocene–lower Eocene sediments on the eastern US Gulf Coastal Plain, modified from Harrington (2003), showing the stratigraphic position of the Red Hot Truck Stop (RHTS) and the Harrell Core. Magnetostratigraphy is from Rhodes et al. (1999), planktic foraminifer zonation of Wade et al. (2011) is based on the data of Mancini and Oliver (1981), and nannoplankton zones of Martini (1971) are from Gibson et al. (1982). RHTS log is from Beard and Dawson (2009). Hatch. represents Hatchetigbee; BCFB represents Bashi Calcareous Fossiliferous Bed; BLM represents Bells Landing Marl; GLM represents Greggs Landing Marl; g represents glauconite; dark gray lithology represents brown, gray siltstone/mudstone; light gray lithology represents glauconitic siltstone and fine sandstone; small dark gray boxes within siltstone represent the presence of fine mud layers throughout; and rounded symbols at base of glauconitic unit represent coarse sand.

Siesser (1983) determined that the Bashi Marl represents calcareous nannofossil zone NP9, perhaps NP10. The NP9 designation for the Bashi Marl is based on the co-occurrence of *Discoaster multiradiatus* and *D. mohleri*, which is stated to be restricted to the late Paleocene. However, Eocene occurrences of *D. mohleri* are known from Demerara Rise, South Atlantic (Mutterlose et al., 2007); Walvis Ridge, South Atlantic (Monechi and Angori, 2006); and Mexico (Garcia-Cordero and Carreño, 2009). The last occurrence of this species is not well constrained. Gibson et al. (1982) dated the Bashi Marl as NP10 based on the occurrence of *Tribrachiatus contortus* and *T. bramlettei*, both of which are restricted to NP10 in the earliest Eocene (Vandenberghe et al., 2012).

Although the PETM has never been positively identified in the GCP using carbon isotope stratigraphy, numerous GCP workers have hypothesized that it would be found near the Tuscahoma–Bashi transition based on bio- and sequence stratigraphy (e.g., Gibson and Bybell, 1994; Dockery, 1998; Harrington et al., 2004). The area around Meridian, MS, including the Red Hot Truck Stop, has been documented as preserving the most complete Tuscahoma–Bashi transition, with the oldest Eocene sediments (Ingram, 1991; Gibson and Bybell, 1994; Harrington, 2003).

Crucially, a lowstand channel termed the T4 sand at the RHTS yields the dinoflagellate cyst *Apectodinium augustum*, as identified by Lucy Edwards (USGS) according to Beard and Dawson (2001). This species is diagnostic of the PETM (e.g., Crouch et al., 2001; Sluijs et al., 2006, 2007b; Harding et al., 2011), and, even though no carbon isotope stratigraphy was available, the T4 sand was therefore assigned to the

PETM by Beard (2008). Based on sequence stratigraphic correlations, Beard (2008) assigned the T4 sand to represent the earliest stages of the PETM because it immediately underlies the Tuscahoma–Bashi boundary: a major unconformity that he ascribes to a eustatic sea level drop during the PETM. Based on this, he argued that the fossil *Teilhardina magnoliana* in the T4 sand represents the oldest primate in North America and revised the patterns of primate migration during the PETM. However, the available evidence suggests that sea level rose during the PETM (Speijer and Morsi, 2002; Sluijs et al., 2008a; Harding et al., 2011), and it remains unclear at which stratigraphic level the onset of the PETM is located at the RHTS or along the GCP in general.

3 Material

We sampled the upper Tuscahoma Fm through Bashi Mb recovered in the Harrell Core (Fig. 1). The paleolatitude of the core during the latest Paleocene and earliest Eocene was $\sim 32^\circ$ N (Boyden et al., 2011). Within the Harrell Core, the Bells Landing Marl lies at 239 m below surface (mbs). The ~ 120 m thick interval between the Bells Landing Marl and the top of the Tuscahoma Fm within the Harrell Core lacks calcareous fossils, as in other sections in the region, and is typified by excellent pollen yields from both the siliciclastic lithologies and interbedded lignites (Harrington et al., 2004; Harrington and Jaramillo, 2007). A ~ 10 cm thick sand-rich and highly micaceous interval occurs at (121.9–121.8 mbs). The overlying uppermost part of the Tuscahoma Fm is rich in siliciclastic sand, mica, and glauconite. The transition to the Bashi Mb lies at ~ 118 mbs, and the calcareous fossiliferous bed of the Bashi Mb starts at ~ 113 mbs; core loss immediately below this fossiliferous unit results in an estimated depth; see Supplement.

4 Methods

Smear slides were made for calcareous nannofossil analyses. Then, samples were freeze-dried and splits were analyzed for total magnetic susceptibility, palynology, and organic geochemistry. Magnetic susceptibility per gram of sediment (MS) was measured using the AGICO KLY-3 device at Utrecht University. Standard palynological treatment was applied for dinocysts and pollen and spore analyses. For the analyses of dinocysts and ratios of marine versus terrestrial palynomorphs, freeze-dried sediment was treated with 30 % HCl and twice with 38 % Hydrofluoric acid (HF) and sieved over a 15 µm nylon mesh. Residues were analyzed at $> 500\times$ magnification. We generally follow the taxonomy of Fensome and Williams (2004); see Supplement for exceptions and a list of encountered species. Materials are stored in the collection of the Laboratory of Palaeobotany and Palynology at Utrecht University. For pollen and spore analyses, approximately 15 grams of sediment was ground in a mortar with pestle and then soaked overnight in HCl to remove any carbonate. These samples were then treated with 40 % HF and left for 3 days to digest silicate minerals before sieving with a 10 µm mesh. Samples were then placed into hot HCl to remove any remaining precipitate before sieving again with a 10 µm mesh. The final stage to remove excess organic matter and any pyrite, was to wash the samples in concentrated HNO_3 for 2 min before a final iteration of sieving. Samples were stained with safranin and then mounted onto coverslips and analyzed at $400\times$ and $1000\times$ phase contrast magnification.

All analyzed samples lacked biogenic carbonate with the exception of the Bashi calcareous fossiliferous bed. We therefore generated δ^{13}C analyses on total organic carbon (TOC). These were performed on decarbonated, freeze-dried samples with a Fison NA 1500 CNS analyzer, connected to a Finnigan Delta Plus mass spectrometer. Analytical precision was better than 0.1 ‰. All values are reported relative to the Vienna Pee Dee Belemnite (VPDB) standard.

For biomarker analyses, powdered and freeze-dried sediments were extracted with a Dionex Accelerated Solvent Extractor using a 9 : 1 (v/v) mixture of dichloromethane and methanol. One aliquot of the extract was separated into apolar and polar fractions. Polar fractions were analyzed using high-performance liquid chromatography/atmospheric pressure chemical ionization–mass spectrometry (Schouten et al., 2007) using an Agilent 1100 HPLC-MSD SL. Single-ion monitoring was used to quantify the abundance of glycerol dialkyl glycerol tetraethers (GDGTs). We apply the TEX_{86}^{H} sea surface temperature (SST) core top calibration, which has a calibration error of 2.5 °C, as this is recommended for (sub)tropical oceans (Kim et al., 2010). We have also calculated TEX_{86}^{L} values following a recent suggestion that this calibration may provide more realistic results for shallow marine sections (Taylor et al., 2013).

The distribution of the branched GDGTs, produced by soil bacteria, is a measure for mean annual air temperature (MAAT) using the methylation of branched tetraether–cyclization of branched tetraether (MBT–CBT) proxy (Weijers et al., 2007). We applied both the MBT–CBT calibration of Weijers et al. (2007) and the MBT′–CBT calibration of Peterse et al. (2012), which yield calibration errors of ~ 5 °C. We also determined the abundances of the branched relative to the isoprenoid tetraethers (BIT index), a proxy for the amount of river-derived soil organic matter versus marine organic matter (Hopmans et al., 2004). An aliquot of the polar fraction was desulfurized using Raney nickel (Sinninghe Damsté et al., 1988) and subsequently separated into polar and apolar fractions. Apolar fractions were hydrogenated using PtO_2 / H_2 and analyzed by gas chromatography (Agilent 6890), gas chromatography–mass spectrometry (ThermoFinnigan DSQ) and gas chromatography–isotope ratio mass spectrometry (ThermoFinnigan Delta V coupled to an Agilent 6890).

All raw data are included in Supplement Table S1.

5 Results and discussion

5.1 Stratigraphy of the Harrell Core

At ∼ 121.9 mbs, the $\delta^{13}C_{TOC}$ records a negative step. Below this level, average values are −25.5 ‰ ($1\sigma = 0.25$), while above it to 118.6 mbs, values average −27.5 ‰ ($1\sigma = 0.70$), with minimum values of −28.6 ‰ (Fig. 3). The onset of this carbon isotope excursion (CIE) corresponds to a ∼ 10 cm thick sand-rich and highly micaceous interval. Because this CIE could theoretically reflect an increase in the relative abundance of marine organic matter over terrestrial organic matter (Sluijs and Dickens, 2012), we tested if it is also present in specific biomarkers. We did not record biomarkers, such as long-chain *n* alkanes, in quantities sufficient for isotope analyses in the apolar fractions of the total lipid extract. The polar fractions, however, yielded sulfur-bound phytane, derived from algal chlorophyll (Brassell et al., 1986; Schoon et al., 2011) and sulfur-bound C_{29} sterane, likely derived from algal C_{29} sterols (Volkman, 1986). These are unlikely derived from land since terrestrial biomarkers are not bound to S as sulfurization requires fresh functionalized molecules (e.g., Sinninghe Damsté et al., 1988). Although the abundance of these biomarkers was insufficient for isotope analyses in many samples, particularly below 121.9 mbs, and results are based on low yields resulting in high standard deviations for the measurements, we reproduce the shift towards lower $\delta^{13}C$ in both sulfur-bound compounds. Concomitantly at 121.9 mbs, abundances of *Apectodinium* spp. increase from ∼ 30 to 80 % of the dinocyst assemblage. Abundances below this level should be considered rough estimates; samples are dominated by terrestrial material, which complicates robust quantitative dinocyst analyses (see below). At the same level, both the TEX_{86} and MBT–CBT paleothermometers (Fig. 3), as well as the influx of abundant pollen derived from thermophilic plants (Fig. 4; see Sect. 5.4), record extreme warming. The combined information unambiguously indicates the presence of a hyperthermal.

We can exclude that the CIE in the Harrell Core reflects any of the hyperthermals younger than that of the PETM. In the overlying calcareous fossiliferous bed of the Bashi Mb, we record the presence of the calcareous nannofossils *Toweius eminens*, *Neochiastozygus junctus*, *Discoaster multiradiatus*, and *Chiasmolithus solitus*, along with the absence of *Discoaster diastypus* (late NP10) and a few *Fasciculithus* specimens (Table S1). This confirms an age of NP10 (Perch-Nielsen, 1985; Bralower, 2005; Young et al., 2011; Vandenberghe et al., 2012), which predates the Eocene Thermal Maximum 2 by ∼ 200 kyr (Lourens et al., 2005). Thus, the hyperthermal in the Harrell Core must be the PETM.

The sandy, micaceous bed at the base of the CIE (121.9–121.8 mbs) marks a distinct peak in MS, and a significant lithological change, interpreted to reflect an unconformity (Figs. 2 and 3). Constraints on the time associated with the hiatus are limited since the upper Tuscahoma Fm is poor in age-diagnostic fossils. However, the Bells Landing Marl (at 239 mbs in the Harrell Core) has been regionally dated to calcareous nannoplankton zone NP9. The presence of *Morozovella subbotinae* in the Bells Landing Marl suggests an age maximally ∼ 0.5 Myr older than the PETM (Wade et al., 2011), which is thus the maximum amount of time associated with this hiatus. Because the onset of the PETM occurs within NP9, the minimum possible duration of the hiatus is negligible. Indeed, a previous pollen study recorded long-term warming over this part of the section (Harrington and Jaramillo, 2007), consistent with other climate records on the last hundreds of thousands of years of the Paleocene (Zachos et al., 2008; Bijl et al., 2009), suggesting that the sediment sequence represents a relatively complete latest Paleocene succession. Given that almost 120 m separate the Bells Landing Marl and the CIE, which maximally represent 0.5 Myr, we suspect that the hiatus at the base of the PETM is minor, likely less than 100 kyr. This implies that the section is suitable to quantify the warming and environmental change during the PETM.

The $\delta^{13}C_{TOC}$ record exhibits significant variation within the CIE. A positive spike in $\delta^{13}C_{TOC}$ occurs within the PETM at ∼ 120.5 mbs. In part, this can be explained by an increase in the relative abundance of terrestrial organic matter (Sluijs and Dickens, 2012); this is indicated by a concomitant rise in BIT index values, suggesting elevated input of soil organic matter, and abundances of terrestrial palynomorphs (Fig. 3; see below). The palynology does not show a large component of reworked specimens, but it is possible that a large component of the organic matter is allochthonous. TOC content is low (Fig. 3), so that enhanced degradation of marine organic matter might have increased $\delta^{13}C_{TOC}$ values (Sluijs and Dickens, 2012) as well as BIT index values (Huguet et al., 2008). We cannot fully explain the positive spike within the CIE, but it must represent a local phenomenon. The interval is rich in siliciclastic sand and mica, pointing to a time interval of nondeposition (winnowing), erosion, or, given the high abundances of terrestrial organic matter and the coarser grains, a storm deposit.

The top of the CIE corresponds to the Tuscahoma–Bashi contact at ∼ 118.8 mbs, which is reflected in a drop in MS (Fig. 3) and represents the widely recognized regional unconformity on the GCP (Gibson and Bybell, 1994). None of our records indicate the presence of the recovery interval, implying that the PETM is only partly present in the Harrell Core. Because the entire recovery interval was apparently truncated by the upper sequence boundary, the PETM sediments were likely deposited during the first part (or body) of the PETM (∼ 80 kyr, Röhl et al., 2007; Murphy et al., 2010). It remains unclear which portion of the first 80 kyr of the CIE is present. The beginning of the PETM might be truncated in the underlying unconformity. However, analyses of thin sections indicate that the ubiquitous glauconite grains are angular (Fig. 5), implying that they were formed in situ. It is estimated that glauconite requires a residence time at the sediment–water

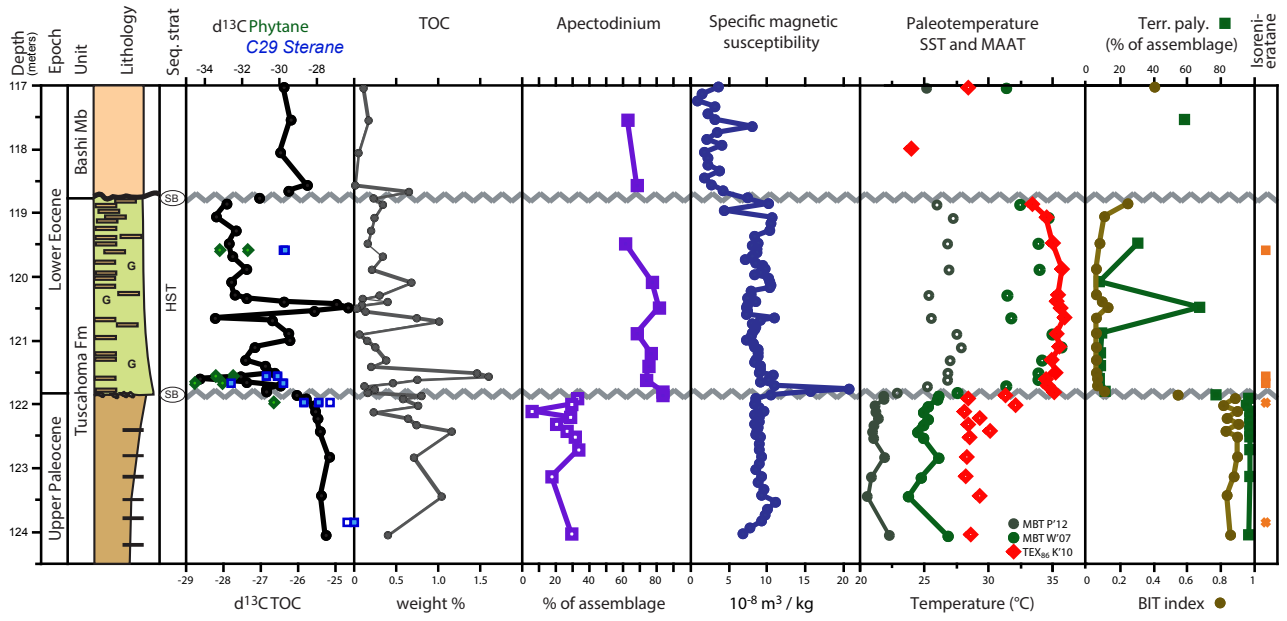

Figure 3. Paleontological and geochemical records across the PETM in the Harrell Core. Schematic lithological units represent the (in brown) upper Paleocene heterogeneous brown, gray siltstone/mudstone; the (in green) PETM glauconitic (G) sands and silts; and the (in light brown) early Eocene siliciclastics of the lower Bashi Mb. Small dark brown boxes within siltstone represent the presence of fine mud layers throughout; rounded symbols at base of glauconitic unit represent coarse sand. Light-colored and open symbols in the $\delta^{13}C$ values of sulfur-bound phytane and sulfur-bound C_{29} sterane yield a relatively high uncertainty of ~ 1 and ~ 1.5 ‰ in isotope values, respectively, due to the low abundance of these compounds in the sediments. Upper Paleocene *Apectodinium* abundances (open squares) should be considered rough estimates; average Paleocene values are 27 % (see text and Supplement Table S1). Calibration-related errors on absolute temperatures for TEX_{86} and MBT–CBT temperatures are 2.5 and 5 °C, respectively. Open TEX_{86} (diamonds) and MBT (circles) symbols indicate temperatures that may be biased by high supply of terrestrial lipids or in situ production, respectively (see text). Pollens and spores versus dinocysts dominantly determine the ratio of terrestrial versus marine palynomorphs. Crosses at isorenieratene indicate intervals where this biomarker was not recorded.

interface of 1000 to 10 000 years to develop (Prothero and Schwab, 2004). This implies that sedimentation rates in this interval were very low and that a significant portion of the body of the CIE is present in the record.

5.2 Implications for regional mammal stratigraphy

The new stratigraphic constraints have direct implications for inferences regarding primate migrations during the PETM. The discovery of the tiny primate *Teilhardina magnoliana* was reported from the T4 sand at the RHTS (Fig. 2, Beard, 2008), which is ~ 10 km north-northeast of the Harrell site. The T4 sand represents the uppermost part of the Tuscahoma Fm at the RHTS, and was suggested to have been deposited during the earliest part of the PETM by Beard (2008). However, it resides on top of the glauconitic unit that is lithostratigraphically analogous to the one representing the PETM in the Harrell Core (Fig. 2). Although carbon isotopic data are not available for the RHTS, the deposition of in situ glauconite therefore implies that significant parts of the PETM underlie the T4 sand at the RHTS. This excludes that the T4 sand represents the earliest stages of the PETM. With the current data set, we cannot estimate the time between the onset of the CIE and the T4 sand at the RHTS, but it likely involved tens of millennia. The first occurrence of primate fossils in the Bighorn Basin is in a paleosol dated to ~ 25 kyr after the onset of the CIE (Smith et al., 2006; Abdul Aziz et al., 2008). This may or may not be earlier than *T. magnoliana* on the GCP.

5.3 Temperature

Both the TEX_{86} and MBT–CBT paleothermometers show a marked warming across the onset of the PETM, of 6 and 5–8 °C, respectively (Fig. 3). We calculated SSTs from isoprenoid GDGTs using various TEX_{86} calibrations (Table S1). We prefer the TEX_{86}^{H} SST core top calibration as this is recommended for (sub)tropical oceans (Kim et al., 2010). TEX_{86}^{H} has a calibration error of 2.5 °C. Despite the recent suggestion that TEX_{86}^{L} may better represent marginal marine regions (Taylor et al., 2013), this calibration results in unrealistically (Keating-Bitonti et al., 2011; Sessa et al., 2012b) low SSTs of ~ 15 °C in the Paleocene and ~ 25 °C during the PETM (Supplement Table S1) and is therefore not further considered. TEX_{86}^{H} indicates late Paleocene SSTs averaging 29 °C ($1\sigma = 1.2$), ~ 5 °C warmer than modern

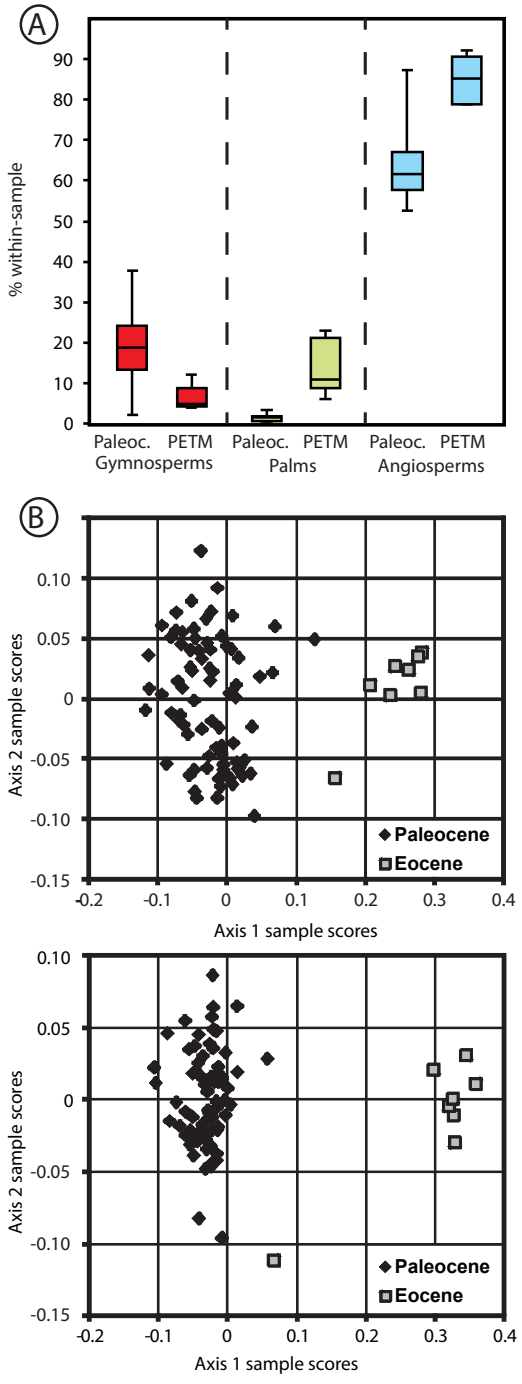

Figure 4. Pollen and spore results. **(A)** Box-plot comparisons between average (mean) within-sample abundance of pre-PETM samples ($n = 77$) from Harrington and Jaramillo (2007) and PETM samples ($n = 8$) from the Tuscahoma Fm of the Harrell Core. Abundances are expressed as average percent within sample. All comparisons between pre-PETM abundances and PETM abundances are statistically significant. **(B)** Non-metric multidimensional scaling plots illustrating pollen compositional differences in the Tuscahoma Fm in the Harrell Core, based on the relative abundance data (top) and on presence–absence data (bottom). While the former reflects changes in dominant taxa, the latter is sensitive to changes in the co-occurrence patterns of taxa within samples.

SSTs in this region. Absolute temperature estimates based on TEX_{86} may, however, be compromised due to the large supply of soil tetraether lipids, as indicated by high BIT values (Weijers et al., 2006). In this uppermost Paleocene interval, higher BIT values correspond to relatively low TEX_{86} values ($R^2 = 0.69$), suggesting that SSTs could be underestimated. On the other hand, TEX_{86} SSTs are slightly higher than mean estimates of 25.5 °C (seasonal range from 23.5 to 27.5 °C) derived from the oxygen isotopic composition of bivalve shells within the lower Eocene marine incursion of the Bashi (Sessa et al., 2012b), and are the same as TEX_{86} temperature estimates from a stratigraphically younger early Eocene bed within the Hatchetigbee Fm (Keating-Bitonti et al., 2011), indicating they represent realistic values.

Based on MBT–CBT, upper Paleocene MAATs were 26.4 °C ($1\sigma = 0.8$) and 21.4 °C ($1\sigma = 0.5$) following the Weijers et al. (2007) and Peterse et al. (2012) calibrations, respectively (Fig. 3). Such temperatures agree with the tropical–pantropical character of the vegetation as recorded from plant macrofossils in the lowermost Eocene lowstand deposits overlying the T4 sand at the Red Hot Truck Stop (Call et al., 1993; Danehy et al., 2007). Quantitatively, the MAAT estimate based on the Weijers calibration corresponds remarkably well to previous MBT–CBT estimates from the stratigraphically younger bed within the Hatchetigbee Fm (Keating-Bitonti et al., 2011) and estimates based on late Paleocene plant leaves in the region (27 °C; Wolfe and Dilcher, 2000). Given the relatively large uncertainties in estimating absolute temperature from both leaves and biomarkers, even the MAATs implied by the Peterse et al. (2012) calibration are within error of the leaf-based estimate. However, we consider the MAAT estimate from the Weijers et al. (2007) calibration to be more realistic for this area and time interval, because of the abovementioned consistency with other proxy data.

Average PETM SSTs based on TEX_{86}^{H} were 35 °C ($1\sigma = 0.7$). This implies a PETM warming of ∼ 6 °C, or slightly less given the potential bias towards lower values in the upper Paleocene due to the contribution of soil GDGTs (see above). MAAT rose by ∼ 8–9 to 35 °C ($1\sigma = 1.4$) based on the Weijers et al. (2007) calibration and by ∼ 5 to 26.6 °C ($1\sigma = 0.9$) following the Peterse et al. (2012) calibration. Because of the low relative abundance of terrestrial lipids in these sediments (indicated by low BIT index values) there is some uncertainty in absolute MBT–CBT temperature estimates due to potential in situ production of the lipids used in the MBT proxy (Peterse et al., 2009). Still, recent regional climate modeling experiments indicated that mean annual SSTs should be similar to MAAT along the GCP margin during this time period (Thrasher and Sloan, 2009), which is consistent with our data. Considering that methods to reconstruct temperature from biomarkers currently yield significant uncertainties, the magnitude of MAAT and SST warming was likely on the order of 5–8 °C.

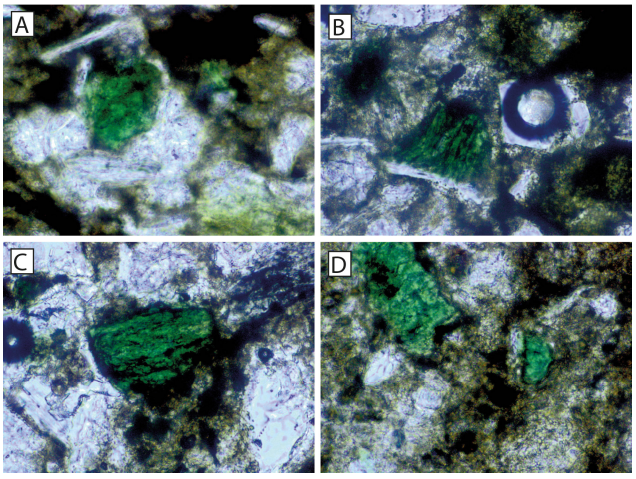

Figure 5. Microphotographs of glauconite grains in thin sections, **(A)** from 121.36 mbs, **(B)** from 120.80 mbs, and **(C)** and **(D)** from 119.68 mbs.

Proxy records of continental air and sea surface temperature across the late Paleocene to the first ∼ 80 kyr of the PETM are available from at least 10 locations. These sites are spread across the globe, and all indicate a 4 to 8 °C warming (Fig. 6), the global average being close to 4–5 °C (Dunkley Jones et al., 2013). Deep-ocean temperatures increased by a similar amount (e.g., Thomas and Shackleton, 1996; Tripati and Elderfield, 2005). Although records from tropical regions are rare, there is no evidence for polar amplification of warming and only little spatial variability in temperature trends. This suggests relatively little change in global atmospheric and oceanic circulation patterns and ocean–atmosphere heat transport during the PETM.

Absolute latest Paleocene and early Eocene land and seawater temperatures of 25 to 29 °C reconstructed here and in the region (Wolfe and Dilcher, 2000; Keating-Bitonti et al., 2011; Sessa et al., 2012b) are relatively modest as compared to other mid- and high-latitude sites (Sluijs et al., 2006; Zachos et al., 2006; Sluijs et al., 2011; Dunkley Jones et al., 2013). A simulation with a current-generation, fully coupled climate model designed to represent early Eocene climates projects GCP SSTs about 5 °C warmer than our proxy estimates (Huber and Caballero, 2011). The simulation also underestimates polar temperatures. Crucially, however, taking into account uncertainties in proxy estimates, such recent simulations (Huber and Caballero, 2011; Lunt et al., 2012) now approach the low meridional temperature gradients found by proxy data during the early Eocene and the PETM.

5.4 Terrestrial vegetation

We combine previously published (Harrington et al., 2004) and new data from the Harrell Core to study vegetation changes during the PETM (see Supplement Table S1 for sampling details). In summary, a significant shift in palynofloral composition is recorded in the Harrell Core between 121.97 and 121.72 m, coinciding with the onset of the CIE: (i) changes in the relative abundance of range-through taxa, (ii) changes in the co-occurrence of taxa in individual samples, (iii) the first occurrence of key Eocene marker taxa, and (iv) the presence of a transient flora with unique elements that are not observed at any time in the Paleocene or Eocene on the US Gulf Coast. These features are all consistent with an excursion flora observed in the Bighorn Basin of Wyoming (Wing et al., 2005; Wing and Currano, 2013).

The eight samples from the uppermost Tuscahoma Fm (121.72 to 118.69 m) contain abundant palm pollens (*Arecipites, Proxapertites operculatus, P. psilatus*, and *Calamuspollenites eocenicus*) along with significant components of other monocots such as the *Sparganiaceae* (bur reeds). Below 121.72 m palm pollens average 1 %, but from 121.72 to 118.69 m this increases to an average within-sample abundance of 13 % (Fig. 4a), which was found to be a statistically significant difference using a Mann–Whitney U test ($U_{77,8} = 0$, $p < 0.0001$). Gymnosperms of all groups decrease in abundance (Fig. 4a) or are absent, including the *Metasequioa/Glyptostrobus* pollen that is otherwise very abundant throughout many lower Paleogene pollen assemblages (Harrington et al., 2004; Harrington and Jaramillo, 2007). This within-sample decrease during the PETM is statistically significant ($U_{77,8} = 48$, $p < 0.0001$). Juglandaceae pollen belonging to *Carya* (hickories) and *Momipites* is rare, although angiosperm pollen increases significantly within the PETM ($U_{77,8} = 16$, $p < 0.0001$) from 64 % in an average Paleocene sample to 85 % in a typical PETM sample (Fig. 4). This is also consistent with the pattern seen in Wyoming (Wing et al., 2005; McInerney and Wing, 2011). Increased abundance within the PETM is recorded for *Porocolpopollenites ollivierae* (belonging to a tropical family: Apocynaceae, Meliaceae, or Styracaceae) together with many other taxa of unknown systematic affinity such as *Nudopollis terminalis* (a normapolle), *Thomsonipollis expolitus* (a normapolle but abundant), and different types of undescribed, new tricolporate pollen.

First occurrences include *Platycarya platycaryoides*, *Platycarya swasticoides*, *Interpollis microsupplingensis*, and *Brosipollis* sp., which were also all previously documented in the uppermost Tuscahoma Fm at the Red Hot Truck Stop (Harrington, 2003). In addition, we record the first occurrence of *Ulmipollenites undulosus*, another feature of the Eocene (Frederiksen, 1998). Taxa that are considered to be transient include *Retistephanocolporites*, which has only ever been recorded previously from uppermost Tuscahoma sediments at Red Hot Truck Stop (Harrington, 2003); plate

1, Fig. 32). Three common transient taxa are a large variety of *Milfordia* (member of the monocot Flagellariaceae, or Restionaceae families); a type of *Ailanthipites* sp. that is large, clearly striate, and not *Ailanthipites berryi*; and a very abundant type of tetracolporate, small striate/reticulate, oblate to spherical pollen grain that is not found anywhere else. There are other taxa that have first appearances within this interval; however, because they are not abundant they cannot be confidently considered as first (and only) occurrences. Several important taxa that are thought to go extinct at the Paleocene–Eocene boundary on the US Gulf Coast (Harrington, 2001; Harrington and Jaramillo, 2007) are not found in this interval (i.e., above 121.97 m), including *Holkopollenites chemardensis, Lanagiopollis cribellatus, Lanagiopollis lihokis* and *Spinaepollis spinosus*.

There are significant differences between the PETM samples from 121.72 to 118.69 m in the Harrell Core and those immediately below in the upper Tuscahoma Fm as described by Harrington and Jaramillo (2007). We carried out nonmetric multidimensional scaling ordination to illustrate changes in relative abundance and in presence–absence (top and bottom plots, respectively, in Fig. 4b). For the relative abundance ordinations, only taxa that are represented by 50 or more specimens within the whole data set of the Harrell Core were included. These samples predominantly represent brackish water to very shallow marine environments, and all lignites and carbonaceous shales have been removed from the sample set before ordination. Relative abundance changes reflect a decrease in Juglandaceae pollen, all gymnosperms, and myricaceous pollen, and an increase of palms, other monocots, and abundant transient taxa in the Eocene (Fig. 4b top). The ordination of presence–absence data (Fig. 4b bottom) reflects changes in co-occurrence patterns and the complete turnover of community membership in the uppermost Tuscahoma Fm. The latter ordination is performed on taxa that are represented by two or more occurrences in two or more different samples.

5.5 Depositional environment and sea level

5.5.1 Upper Paleocene

Terrestrial palynomorphs, notably angiosperm pollens, comprise > 95 % of the palynomorphs in the uppermost Paleocene (125–121.9 mbs), cuticle fragments of terrestrial plant leaves are abundant, small wood fragments are present, and BIT values are high (> 0.8). In (sub)tropical, relatively humid settings such as the GCP in the Paleocene (e.g., Harrington and Kemp, 2001), angiosperm pollen and terrestrial GDGTs are documented as being transported to the ocean by rivers (Hopmans et al., 2004; Moss et al., 2005).

We recorded marine dinoflagellate cysts in all samples, but quantification of assemblages is difficult due to dilution by terrigenous matter. Dinocyst abundances in the upper Paleocene interval are therefore based on relatively low counts (between 10 and 60 cysts) and should therefore be considered as rough estimates. Assemblages are typical for early Paleogene marginal marine deposits. Averaged over the entire interval (238 cysts), *Apectodinium* spp. (27 %, some with minor morphological deviations from the type species; see Supplement) and the *Senegalinium* complex (*sensu* Sluijs and Brinkhuis, 2009; 20 %) are abundant. The *Senegalinium* cpx. in the Harrell Core almost exclusively comprises *Senegalinium* spp., but includes sporadic *Phthanoperidinium* spp. and *Deflandrea* spp. The *Senegalinium* cpx., and *Senegalinium* spp., represents a group of taxa derived from dinoflagellates known to have been tolerant to low-salinity waters, based on empirical information (Harland, 1973; Brinkhuis et al., 2006; Sluijs and Brinkhuis, 2009; Sluijs et al., 2009; Harding et al., 2011). Moreover, *Eocladopyxis* spp. are present (2 %), and modern representatives of this family (Goniodomidae) are successful in very nearshore and lagoonal settings, partly due to their euryhaline ecology (Zonneveld et al., 2013). Other consistently present dinocyst taxa include typical shelf dwellers such as members of the *Cordosphaeridium fibrospinosum* cpx. (*sensu* Sluijs and Brinkhuis, 2009) (16 %), the *Areoligera–=Glaphyrocysta* cpx. (8 %), *Operculodinium* spp. (8 %), and *Spiniferites* spp. (6 %). Another important aspect of the palynological assemblage is the consistent presence of the freshwater alga *Pediastrum*. The combined palynological and biomarker information therefore implies that during the latest Paleocene the Harrell Core locality was a very nearshore environment, perhaps a lagoon with significant river runoff, which is in agreement with the lithological information.

Apectodinium was much more abundant on the GCP in the latest Paleocene than at mid- and high-latitude sections (e.g., Heilmann-Clausen, 1985; Harding et al., 2011; Sluijs et al., 2011). *Apectodinium* was globally abundant during the PETM, suggesting that late Paleocene conditions on the GCP were analogous to those developing on a global scale during the PETM. The ecology of *Apectodinium*, as well as the critical factors triggering its widespread dominance during the PETM, remains puzzling. *Apectodinium* tolerated a large salinity range, and likely preferred relatively eutrophic and warm conditions, but its global success remains hard to explain (e.g., Sluijs et al., 2007b; Sluijs and Brinkhuis, 2009). Upper Paleocene assemblages within the Harrell Core contain 27 % *Apectodinium*, a value close to that recorded at several high-latitude sites during the PETM (Sluijs et al., 2006, 2011). Whatever environmental or biotic factors triggered the global spread of this taxon during the PETM must have been common to both low- and high-latitude areas.

5.5.2 PETM

By contrast to the upper Paleocene, PETM sediments dominantly yield marine palynomorphs and low BIT values (< 0.1). The concomitant change in lithology from silts and muds to angular glauconite-rich sands and silts

indicates sedimentary condensation. Along with the dominant *Apectodinium* spp. (between 60 and 85 %), only *Diphyes colligerum* (between 1 and 18 %) and the *Areoligera–Glaphyrocysta* cpx. (3–14 %) are common during the PETM. *Cordosphaeridium fibrospinosum* cpx. and *Spiniferites* spp. (6 %) are consistently present in low abundances. Notably, the *Senegalinium* cpx. and *Eocladopyxis* spp. are mostly absent. The absence of the lagoonal to inner neritic components of the dinocyst assemblage, combined with a massive decrease in the abundance of terrestrial pollens, spores, and biomarkers, support an increase in the distance of the site to shore. Common to abundant occurrences of the *Areoligera–Glaphyrocysta* cpx. (here overwhelmed by the *Apectodinium* acme) have also previously been linked to transgression (Iakovleva et al., 2001; Sluijs et al., 2008a). The combined information is consistent with sea level rise during the PETM along the GCP. Because our proxies qualitatively assess distance to shore, we cannot estimate the magnitude of sea level rise.

Relative sea level rise is consistent with many marginal marine sedimentary records worldwide (e.g., Speijer and Morsi, 2002; Harding et al., 2011, Fig. 6), and indicate PETM-related eustatic rise (e.g., Sluijs et al., 2008a). Similar to our study, not many studies have estimated the magnitude of sea level rise since most proxies do not necessarily record water depth but rather the coast or habitat changes that are related to sea level fluctuations (e.g., Jorissen et al., 1995; Sluijs et al., 2008a). Sluijs et al. (2008a) speculated that during the PETM, sea level could have risen a maximum of 30 m if several independent mechanisms were combined, including tectonism, steric effects, and a small ice sheet. However, it may be argued that only steric effects contributed; the temperature–density relationship of seawater (1.9×10^{-2} % volume $^{\circ}C^{-1}$) implies a modest sea level rise of 3–5 m rise from the $\sim 5\,^{\circ}C$ ocean warming (Sluijs et al., 2008a). However, the depth gradient from the coast to the shelf–slope break was likely much less in the Eocene than at present due to the long-term absence of large variations in continental ice volume (Sømme et al., 2009). Therefore, even a relatively small rise in global average sea level would have resulted in a large landward shift of the coastline, explaining the response in sedimentary data as compiled in Fig. 6.

Previous studies suggested that the PETM was absent from sections along the US margin because of a concurrent drop in sea level (Gibson and Bybell, 1994; Beard, 2008). However, our results indicate that the PETM was deposited during a highstand in this region (Fig. 3). The overlying Bashi Mb has an erosional contact with the Tuscahoma. This suggests that PETM sediments were deposited widely on the GCP but subsequently eroded during a sea level drop in the earliest Eocene. This explains the unconformable upper bound of the PETM in the Harrell Core, as well as the absence of the PETM at many locations along the GCP. Moreover, it is consistent with patterns described from many other shelf sections worldwide, such as New Jersey and the North Sea (e.g., Sluijs et al., 2008a).

Although regional sea level fluctuations need not correspond to global trends, the recorded eustatic rise complicates the hypothesis that a drop in sea level facilitated intercontinental mammal migrations during the PETM. More likely, poleward expansion of climate zones set the stage for these migrations (e.g., Bowen et al., 2002).

5.6 Ocean deoxygenation

Within the PETM we recorded sulfur-bound isorenieratane (Fig. 3), a derivative of the carotenoid isorenieratene, in similar concentrations to sulfur-bound phytane and C_{29} sterane. This chemical fossil is derived from the brown strain of photosynthetic green sulfur bacteria, which requires euxinic (anoxic and sulfidic) conditions (Sinninghe Damsté et al., 1993). We did not record it in the upper Paleocene. Given that organic matter preservation conditions were better then (sediments are finer grained and TOC content is higher in the Paleocene than in the PETM; Fig. 3), isorenieratene was likely not produced at the site during the late Paleocene. Despite the limited available data points, the presence of isorenieratene indicates that photic-zone euxinia developed along the Gulf margin during the PETM. Curiously, while euxinic conditions developed in the photic zone, glauconite was forming on the seafloor, and organic linings of benthic foraminifera (Supplement Table S1) are present in the palynological residue, suggesting that the seafloor was oxygenated. The combined information allows for several scenarios to explain this paradox. (1) The lower photic zone but not the seafloor was anoxic. We consider this unlikely because in modern marine environments the sulfide in the water column is almost always formed in the underlying anoxic and sulfidic sediment (e.g., Yao and Millero, 1995). (2) Isorenieratane was transported from euxinic environments further inshore. This mechanism has been proposed previously for other time intervals but is generally considered unlikely (Sinninghe Damsté and Hopmans, 2008) because isorenieratene is among the most labile forms of organic carbon and requires anoxic conditions and short transport time and trajectories to preserve in sediments (Harvey, 2006). (3) The foraminifer linings were transported to the site and concentrated due to sea level rise and sediment starvation, while isorenieratene was produced in the water column at the Harrell Core site. This mechanism cannot be excluded with the present data. However, benthic foraminifer linings are relatively susceptible to oxic degradation and are therefore unlikely to be preserved in an oxic environment during lateral transport. (4) Euxinic conditions developed intermittently, most probably seasonally, within the photic zone in the water column, or, given the limited paleodepth of the study site, on a sun-lit seafloor. The co-occurrence of benthic fauna and photic zone euxinia has previously been attributed to seasonal, decadal, or century timescale variations in water

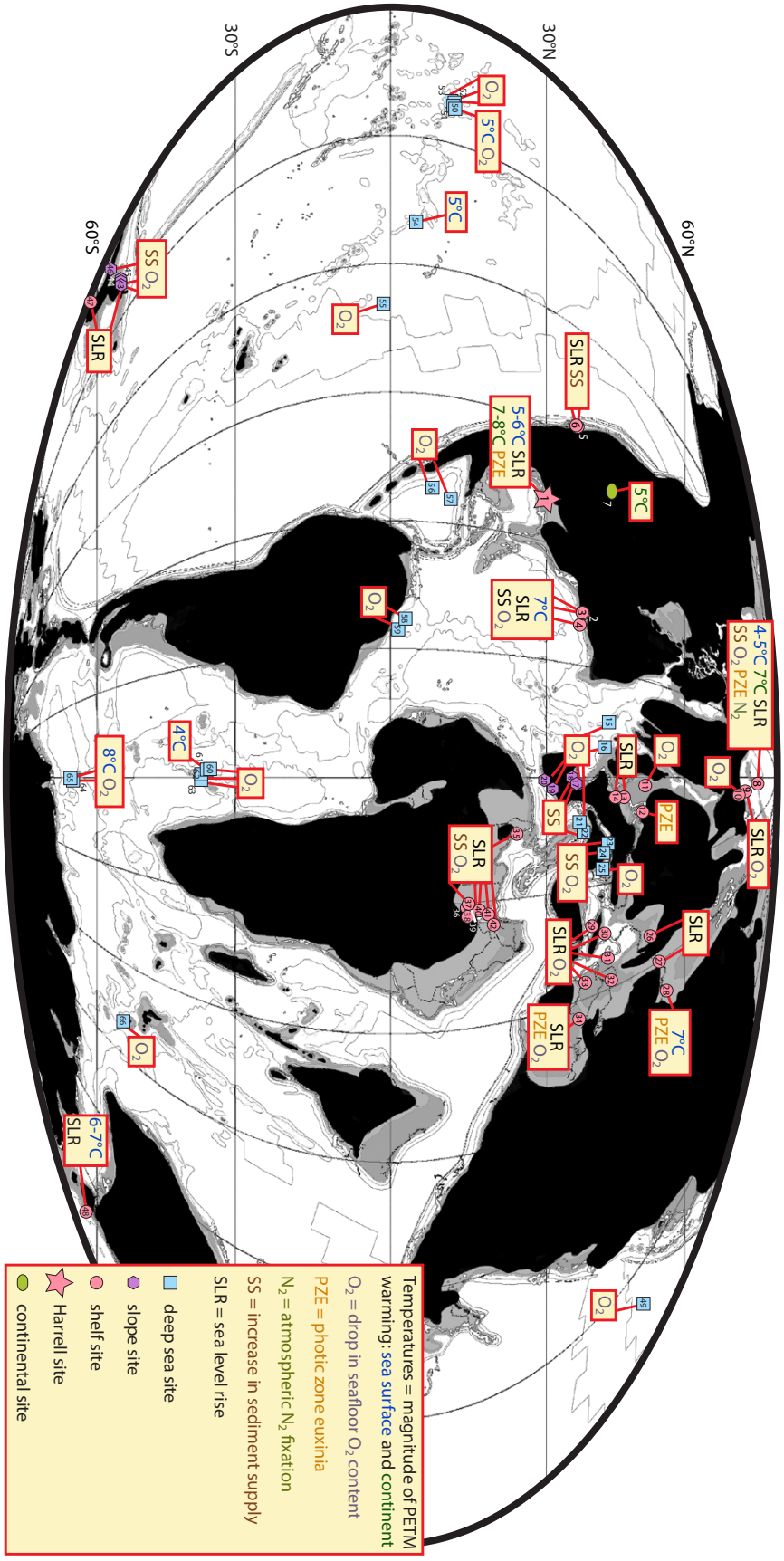

Figure 6. Records of relative changes in SST (blue), continental MAAT (green), decreases in seafloor O_2 content (O_2), photic zone euxinia (PZE), atmospheric nitrogen fixation (N_2), sea level rise (SLR), and increasing siliciclastic sediment supply (SS) on a paleogeographic map (modified from Markwick, 2007) during the PETM. Star indicates the location of the Harrell Core (no. 1). See Supplement and Table S2 for site information and the nature and source of the data. Data interpretations follow the cited paper unless stated otherwise.

column oxygen concentration from euxinic to oxygenated (Kenig et al., 2004). The seasonal development of hypoxia is a common and increasing feature of modern continental margins (Diaz and Rosenberg, 2008). We consider scenario 4 to be the most likely, implying that intermittent, likely seasonal, photic zone euxinia developed at the study site.

These results are consistent with published data from other locations where robust proxy data on seafloor oxygen content is available (Fig. 6; Supplement Table S2) (e.g., Dickson et al., 2012; Winguth et al., 2012). However, while the deep sea experienced only a limited reduction in seafloor oxygen (Chun et al., 2010; Pälike et al., 2014), anoxia developed on continental slopes (Nicolo et al., 2010) and shelves (Speijer and Wagner, 2002; Sluijs et al., 2008b). Moreover, at several coastal shelf sites isorenieratene or derivatives thereof has been observed in the sediment, indicating photic zone euxinia (e.g., Sluijs et al., 2006; Frieling et al., 2014) (Fig. 6). In the modern ocean, the presence of isorenieratene in sediments is restricted to semi-enclosed basins, such as the Black Sea. An increase in anoxic zones in coastal oceans is also consistent with barium records; continental margin anoxia facilitates sulfate reduction, which in turn, promotes barium regeneration from sediments. The barium may subsequently be buried in open-ocean sediments, which is consistent with reconstructions (Paytan et al., 2007).

Widespread euxinic conditions in marginal marine and more open oceanic settings have only been previously documented for so-called "global" oceanic anoxic events during the mid-Cretaceous, early Toarcian, the Permian–Triassic boundary event, and the Frasnian–Fammenian boundary (e.g., Sinninghe Damsté and Köster, 1998; Joachimski et al., 2001; Grice et al., 2005). Interestingly, these events were also associated with warming and massive perturbations of the global carbon cycle, though the timescales involved were substantially longer than those of the PETM and of anthropogenic changes. Given the evidence (Fig. 6), the PETM therefore provides the geologically most recent, and likely the best, example of rapidly expanding, widespread ocean deoxygenation.

Ocean deoxygenation during the PETM was likely generated by processes similar to those contributing to today's so-called "dead zones". Currently, these oxygen-depleted zones are caused by coastal eutrophication, stratification, and warming resulting from anthropogenic activities (Doney, 2010). If methane originating from submarine hydrates was released at the start of the PETM, its oxidation in the ocean should have caused widespread deoxygenation (Dickens et al., 1997). Deep-ocean circulation may have become sluggish at the onset of the event due to changes in climate and an increase in vertical temperature gradients in the ocean, leading to seafloor O_2 depletion (Ridgwell and Schmidt, 2010; Winguth et al., 2012). Moreover, given the temperature dependence of O_2 solubility in seawater, a rapid $\sim 5\,^{\circ}C$ warming should have decreased O_2 solubility by between 15 and 20 %, depending on the background temperature, which could drive already hypoxic regions to anoxia. Crucially, global warming led to an accelerated hydrological cycle, which together with elevated pCO_2 values resulted in increased weathering (John et al., 2012) and at least regionally seasonal intensification of river runoff (Kopp et al., 2009), leading to increased nutrient input and coastal eutrophication. Importantly, increased SSTs in conjunction with an enhanced hydrological cycle strengthened stratification, hampering atmosphere-ocean gas exchange. All these factors, to various degrees, conspired to reduce O_2 concentrations in seawater and allowed for euxinic conditions to develop along coastal margins, although the dominant forcing factor may have been different regionally.

6 PETM continental margin anoxia driven by nutrient feedbacks?

The PETM offers the unique opportunity for the quantification of biogeochemical feedbacks resulting from the rapid expansion of (seasonal) anoxia along the GCP, northern and southern Tethyan margins, the Arctic Ocean, the North Sea, epicontinental Russia and margins in the southwest Pacific Ocean (Supplement Table S2 and references therein). This supports the expansion of global (seasonally) anoxic (Dickson et al., 2012) and hypoxic seafloor, particularly in marginal marine areas. Similar to what is expected for the future ocean, PETM hypoxia and anoxia likely had major effects on nutrient availability and carbon cycling. Sediments overlain by (seasonally) hypoxic and anoxic bottom waters recycle phosphorus (P) from organic matter efficiently (Slomp and Van Cappellen, 2007). On geological timescales, P is likely the limiting nutrient for marine primary production (Tyrrell, 1999). An increase in (seasonal) anoxia along continental margins should therefore have increased P fluxes and thereby coastal productivity; this effect is potentially much larger than that of increased nutrient supply by rivers (Tsandev and Slomp, 2009). Available micropaleontological data, suggesting sustained increased primary productivity in nearshore waters during the PETM (Sluijs et al., 2007a), are consistent with more efficient nutrient cycling. Regional evidence exists for high rates of nitrogen fixation (Knies et al., 2008), which may have compensated for nitrogen loss through denitrification and anaerobic ammonium oxidation (anammox) in the low-oxygen waters (Kuypers et al., 2005). As proposed for mid-Cretaceous oceanic anoxia (Kuypers et al., 2004), this may have been a dominant factor in sustaining high productivity during the PETM.

The duration of enhanced nutrient cycling and deoxygenation is especially important to assess the potential impact on the carbon cycle. Data from most sites point towards (seasonal) anoxia persisting for tens of thousands of years during the PETM (e.g., Gavrilov et al., 2003; Sluijs et al., 2008b; Nicolo et al., 2010). In part, this may reflect the residence time of the injected carbon that provided the key forcing for

the deoxygenation. The residence time of P in the modern ocean is estimated to be between 10 000 and 40 000 years (Slomp and Van Cappellen, 2007). Although data on absolute P fluxes are lacking, a substantial reduction in the efficiency of P burial in shelf sediments would have increased the residence time of P. This can explain why coastal (seasonal) anoxia persisted for a pronounced part of the duration of the body of the PETM ($\sim$ 80 kyr). If this mechanism were active, one would expect high organic carbon burial rates on the shelves during the PETM. Indeed, burial rates of organic carbon significantly increased during the first $\sim$ 80 kyr of the event in many shelf areas including the Tethys (e.g., Bolle et al., 2000; Speijer and Wagner, 2002; Gavrilov et al., 2003), Pacific (John et al., 2008), Arctic (Sluijs et al., 2008b), and Atlantic (see overview in John et al., 2008). Organic carbon burial in marine sediments strongly depends on the supply of sediments (Berner, 1982), so, along with P regeneration, the increase in siliciclastic sediment supply to many shelf areas (Fig. 6) most likely promoted organic carbon burial. Moreover, as sea level rise enlarged the size of the submerged shelves the carbon burial potential increased even further. Even though no climate cooling or recovery of global exogenic $\delta^{13}C$ occurred during this time interval, likely due to continued injection of ^{13}C-depleted carbon (Zeebe et al., 2009), shelves may have represented a significantly enhanced sink of organic carbon during the PETM.

The evolution of ocean oxygen concentrations through the PETM has direct relevance for our understanding of the modern and future ocean. We suggest that the widespread anoxia during the PETM significantly affected nutrient cycles, which in turn acted as an important driver of increased marginal marine productivity and carbon burial. This explains the observed biotic fluctuations, as deduced from assemblages of benthic foraminifers, calcareous nannofossils and dinoflagellate cysts (Sluijs et al., 2007a; Thomas, 2007; Sluijs et al., 2009; Gibbs et al., 2012). The next challenge is to further quantify the changes in nutrient budgets and oxygen concentrations. This knowledge will help to improve mid- to long-term projections of anthropogenic impacts and the resulting transition towards a warmer, high-CO_2, and low-oxygen ocean.

The Supplement related to this article is available online at doi:10.5194/cp-10-1421-2014-supplement.

Acknowledgements. Funding for this research was provided by the Netherlands Organization for Scientific Research (Veni grant 863.07.001 to A. Sluijs and a Vici grant to S. Schouten) and the European Research Council under the European Community's Seventh Framework Programme (Starting Grant no. 259627 to A. Sluijs and Consolidator Grant no. 278364 to C. P. Slomp). Paul Markwick provided his paleogeographic reconstruction. We thank E. Thomas, M. Huber, M. Schaller, A. Riboulleau, and R. Fluegeman for discussions and reviews on the Climate of the Past Discussions forum, which considerably improved this manuscript. We thank several colleagues, including G. R. Dickens for comments on an earlier version of this paper; C. Beard (Carnegie Museum of Natural History, Pittsburgh) for discussions regarding the stratigraphy at the Red Hot Truck Stop; and D. Dockery (Office of Geology at the Mississippi Department of Environmental Quality) for discussions, access to sediment cores, and assistance with sampling. We thank P. de Boer (Utrecht University) for confirming our thin section observations, and A. van Dijk, J. van Tongeren, N. Welters (Utrecht University), E. Hopmans, A. Mets, and J. Ossebaar (Royal NIOZ) for technical support.

Edited by: Y. Godderis

References

Abdul Aziz, H., Hilgen, F. J., van Luijk, G. M., Sluijs, A., Kraus, M. J., Pares, J. M., and Gingerich, P. D.: Astronomical climate control on paleosol stacking patterns in the upper Paleocene – lower Eocene Willwood Formation, Bighorn Basin, Wyoming, Geology, 36, 531–534, doi:10.1130/G24734A.1, 2008.

Baum, G. R. and Vail, P. R.: Sequence stratigraphic concepts applied to Paleogene outcrops, Gulf and Atlantic basins, Special Publication – Society of Economic Paleontologists and Mineralogists, 42, 309–327, 1988.

Beard, K. C.: The oldest North American primate and mammalian biogeography during the Paleocene–Eocene Thermal Maximum, P. Natl. Acad. Sci. USA, 105, 3815–3818, 2008.

Beard, K. C. and Dawson, M. R.: Early Wasatchian mammals from the Gulf Coastal Plain of Mississippi: Biostratigraphic and paleobiogeographic implications, in: Eocene biodiversity: Unusual occurrences and rarely sampled habitats, edited by: Gunnel, G. R., Kluwer Academic/Plenum Publishers, New York, 75–94, 2001.

Beard, K. C. and Dawson, M. R.: Early Wasatchian Mammals of the Red Hot Local Fauna, uppermost Tuscahoma Formation, Lauderdale County, Mississippi, Ann. Carnegie Mus., 78, 193–243, 2009.

Berner, R. A.: Burial of organic carbon and pyrite sulfur in the modern ocean; its geochemical and environmental significance, Am. J. Sci., 282, 451–473, doi:10.2475/ajs.282.4.451, 1982.

Bijl, P. K., Schouten, S., Sluijs, A., Reichart, G.-J., Zachos, J. C., and Brinkhuis, H.: Early Palaeogene temperature evolution of the southwest Pacific Ocean, Nature, 461, 776–779, 2009.

Bijl, P. K., Sluijs, A., and Brinkhuis, H.: A magneto- and chemostratigraphically calibrated dinoflagellate cyst zonation of the early Palaeogene South Pacific Ocean, Earth-Sci. Rev., 124, 1–31, doi:10.1016/j.earscirev.2013.04.010, 2013.

Bolle, M.-P., Pardo, A., Hinrichs, K.-U., Adatte, T., von Salis, K., Burns, S., Keller, G., and Muzylev, N.: The Paleocene-Eocene

transition in the marginal northeastern Tethys (Kazakhstan and Uzbekistan), Int. J. Earth Sci., 89, 390–414, 2000.

Bowen, G. J., Clyde, W. C., Koch, P. L., Ting, S. Y., Alroy, J., Tsubamoto, T., Wang, Y. Q., and Wang, Y.: Mammalian dispersal at the Paleocene/Eocene boundary, Science, 295, 2062–2065, 2002.

Boyden, J. A., Müller, R. D., Gurnis, M., Torsvik, T. H., Clark, J. A., Turner, M., Ivey-Law, H., Watson, R. J., and Cannon, J. S.: Next-generation plate-tectonic reconstructions using GPlates, in: Geoinformatics: Cyberinfrastructure for the Solid Earth Sciences, edited by: Keller, G. R. and Baru, C., Cambridge University Press, 95–114, 2011.

Bralower, T. J.: Paleocene–early Oligocene calcareous nannofossil biostratigraphy, ODP Leg 198 Sites 1209, 1210, and 1211 (Shatsky Rise, Pacific Ocean), in: Proceedings of the Ocean Drilling Program, Scientific Results, 198, edited by: Bralower, T. J., Premoli Silva, I., and Malone, M. J., Ocean Drilling Program, College Station, TX, 1–15, 2005.

Brassell, S. C., Lewis, C. A., de Leeuw, J. W., Lange, F. d., and Sinninghe Damsté, J. S.: Isoprenoid thiophenes: novel products of sediment diagenesis?, Nature, 320, 160–162, 1986.

Brinkhuis, H., Schouten, S., Collinson, M. E., Sluijs, A., Sinninghe Damsté, J. S., Dickens, G. R., Huber, M., Cronin, T. M., Onodera, J., Takahashi, K., Bujak, J. P., Stein, R., van der Burgh, J., Eldrett, J. S., Harding, I. C., Lotter, A. F., Sangiorgi, F., van Konijnenburg-van Cittert, H., de Leeuw, J. W., Matthiessen, J., Backman, J., Moran, K., and the Expedition 302 Scientists: Episodic fresh surface waters in the Eocene Arctic Ocean, Nature, 441, 606–609, 2006.

Call, V. B., Manchester, S. R., and Dilcher, D. L.: *Wetherellia* fruits and associated fossil plant remains from the Paleocene/Eocene Tuscahoma-Hatchetigbee interval, Meridian, MIssissippi, Mississippi Geology, 14, 10–18, 1993.

Chun, C. O. J., Delaney, M. L., and Zachos, J. C.: Paleoredox changes across the Paleocene-Eocene thermal maximum, Walvis Ridge (ODP Sites 1262, 1263, and 1266): evidence from Mn and U enrichment factors, Paleoceanography, 25, PA4202, doi:10.1029/2009pa001861, 2010.

Crouch, E. M., Heilmann-Clausen, C., Brinkhuis, H., Morgans, H. E. G., Rogers, K. M., Egger, H., and Schmitz, B.: Global dinoflagellate event associated with the late Paleocene thermal maximum, Geology, 29, 315–318, 2001.

Danehy, D. R., Wilf, P., and Little, S. A.: Early Eocene Macroflora from the Red Hot Truck Stop Locality (Meridian, Mississippi, USA), Palaeontologia Electronica, 10, 1–31, 2007.

Diaz, R. J., and Rosenberg, R.: Spreading Dead Zones and Consequences for Marine Ecosystems, Science, 321, 926–929, doi:10.1126/science.1156401, 2008.

Dickens, G. R.: Down the Rabbit Hole: toward appropriate discussion of methane release from gas hydrate systems during the Paleocene-Eocene thermal maximum and other past hyperthermal events, Clim. Past, 7, 831–846, doi:10.5194/cp-7-831-2011, 2011.

Dickens, G. R., Castillo, M. M., and Walker, J. C. G.: A blast of gas in the latest Paleocene: Simulating first-order effects of massive dissociation of oceanic methane hydrate, Geology, 25, 259–262, 1997.

Dickson, A. J., Cohen, A. S., and Coe, A. L.: Seawater oxygenation during the Paleocene-Eocene Thermal Maximum, Geology, 40, 639–642, 2012.

Dockery, D. T.: The invertebrate macropaleontology of the Clarke County, Mississippi, area, Mississippi Bureau of Geology, Department of Natural Resources, Jackson, MS, 1980.

Dockery, D. T.: Molluscan faunas across the Paleocene/Eocene series boundary in the North American Gulf Coastal Plain, in: Late Paleocene-early Eocene climatic and biotic events in the marine and terrestrial records, edited by: Aubry, M.-P., Lucas, S. G., and Berggren, W. A., Columbia University Press, New York, 296–322, 1998.

Dockery, D. T., Copeland, C. W., and Huddlestun, P. F.: Reply to a Revision of the Hatchetigbee and Bashi Formations, Mississippi Geol., 4, 11–15, 1984.

Doney, S. C.: The growing human footprint on coastal and open-ocean biogeochemistry, Science, 328, 1512–1516, doi:10.1126/science.1185198, 2010.

Dunkley Jones, T., Lunt, D. J., Schmidt, D. N., Ridgwell, A., Sluijs, A., Valdes, P. J., and Maslin, M.: Climate model and proxy data constraints on ocean warming across the Paleocene-Eocene Thermal Maximum, Earth-Sci. Rev., 125, 123–145, doi:10.1016/j.earscirev.2013.07.004, 2013.

Edwards, L. E. and Guex, J.: Graphic correlation of the Marlboro Clay and Nanjemoy Formation (uppermost Paleocene and lower Eocene) of Virginia and Maryland, in: Palynology: Principles and applications, edited by: Jansonius, J. and McGregor, D. C., American Association of Stratigraphic Palynologists Foundation, College Station, Texas, 985–1009, 1996.

Fensome, R. A. and Williams, G. L.: The Lentin and Williams Index of Fossil Dinoflagellates 2004 Edition, American Association of Stratigraphic Palynologists (AASP) Contribution Series 42, 909 pp., 2004.

Frederiksen, N. O.: Upper Paleocene and lowermost Eocene angiosperm pollen biostratigraphy of the Eastern Gulf Coast and Virginia, Micropaleontology, 44, 45–68, 1998.

Frederiksen, N. O., Gibson, T. G., and Bybell, L. M.: Paleocene-Eocene boundary in the eastern Gulf Coast, T. Gulf Coast Assoc. Geol. Soc., 32, 289–294, 1982.

Frieling, J., Iakovleva, A. I., Reichart, G.-J., Aleksandrova, G. N., Gnibidenko, Z. N., Schouten, S., and Sluijs, A.: Paleocene – Eocene warming and biotic response in the epicontinental West Siberian Sea, Geology, in press, doi:10.1130/G35724.1, 2014.

Galloway, W. E., Ganey-Curry, P. E., Li, X., and Buffler, R. T.: Cenozoic depositional history of the Gulf of Mexico basin, APG Bulletin, 84, 1743–1774, 2000.

Garcia-Cordero, E. and Carreño, A. L.: Upper lower Eocene calcareous nannoplankton from the Las Pocitas core (Tepetate formation), Baja California Sur, Mexico, Rev. Mex. Cienc. Geol., 26, 37–47, 2009.

Gavrilov, Y., Shcherbinina, E. A., and Oberhänsli, H.: Paleocene-Eocene boundary events in the northeastern Peri-Tethys, in: Causes and Consequences of Globally Warm Climates in the Early Paleogene. Geological Society of America Special Paper 369, edited by: Wing, S. L., Gingerich, P. D., Schmitz, B., and Thomas, E., Geological Society of America, Bolder, Colorado, 147–168, 2003.

Gibbs, S. J., Bown, P. R., Murphy, B. H., Sluijs, A., Edgar, K. M., Pälike, H., Bolton, C. T., and Zachos, J. C.: Scaled biotic disruption during early Eocene global warming events, Biogeosciences, 9, 4679–4688, doi:10.5194/bg-9-4679-2012, 2012.

Gibson, T. G.: New stratigraphic unit in the Wilcox Group (upper Paleocene-lower Eocene) in Alabama and Georgia, Stratigraphic notes, 1980–1982, US Geological Survey Bulletin, 1529, H23–H32, 1982.

Gibson, T. G. and Bybell, L. M.: Facies changes in the Hatchetigbee Formation in Alabama-Georgia and the Wilcox-Claiborne group unconformity, T. Gulf Coast Assoc. Geol. Soc., 31, 301–306, 1981.

Gibson, T. G. and Bybell, L. M.: Sedimentary Patterns across the Paleocene-Eocene boundary in the Atlantic and Gulf coastal plains of the United States, B. Soc. Belge Geol., 103, 237–265, 1994.

Gibson, T. G., Mancini, E. A., and Bybell, L. M.: Paleocene to middle Eocene stratigraphy of Alabama, T. Gulf Coast Assoc. Geol. Soc., 32, 289–294, 1982.

Grice, K., Cao, C., Love, G. D., Böttcher, M. E., Twitchett, R. J., Grosjean, E., Summons, R. E., Turgeon, S. C., Dunning, W., and Jin, Y.: Photic Zone Euxinia During the Permian-Triassic Superanoxic Event, Science, 307, 706–709, 2005.

Harding, I. C., Charles, A. J., Marshall, J. E. A., Pälike, H., Roberts, A. P., Wilson, P. A., Jarvis, E., Thorne, R., Morris, E., Moremon, R., Pearce, R. B., and Akbari, S.: Sea-level and salinity fluctuations during the Paleocene-Eocene thermal maximum in Arctic Spitsbergen, Earth Planet. Sc. Lett., 303, 97–107, 2011.

Harland, R.: Dinoflagellate cysts and acritarchs from the Bearpaw Formation (Upper Campanian) of southern Alberta, Canada, Palaeontology, 16, 665–706, 1973.

Harrington, G. J.: Impact of Paleocene/Eocene Greenhouse Warming on North American Paratropical Forests, Palaios, 16, 266–278, 2001.

Harrington, G. J.: Wasatchian (Early Eocene) pollen floras from the Red Hot Truck Stop, Mississippi, USA, Palaeontology, 46, 725–738, 2003.

Harrington, G. J. and Jaramillo, C. A.: Paratropical floral extinction in the Late Palaeocene-Early Eocene, Palaeontology 46, 725–738, 2007.

Harrington, G. J. and Kemp, S. J.: US Gulf Coast vegetation dynamics during the latest Palaeocene, Palaeogeogr. Palaeocl., 167, 1–21, 2001.

Harrington, G. J., Kemp, S. J., and Koch, P. L.: Palaeocene-Eocene paratropical floral change in North America: Responses to climate change and plant immigration, J. Geol. Soc., 161, 173–184, 2004.

Harvey, H. R.: Sources and cycling of organic matter in the marine water column, in: Marine Organic Matter. The Handbook of Environmental Chemistry 2N, edited by: Volkman, J. K., Springer, Berlin, Germany, 1–25, 2006.

Heilmann-Clausen, C.: Dinoflagellate stratigraphy of the Uppermost Danian to Ypresian in the Viborg 1 borehole, Central Jylland, Denmark, DGU A7, 1–69, 1985.

Hopmans, E. C., Weijers, J. W. H., Schefuß, E., Herfort, L., Sinninghe Damsté, J. S., and Schouten, S.: A novel proxy for terrestrial organic matter in sediments based on branched and isoprenoid tetraether lipids, Earth Planet. Sci. Lett., 224, 107–116, 2004.

Huber, M. and Caballero, R.: The early Eocene equable climate problem revisited, Clim. Past, 7, 603–633, doi:10.5194/cp-7-603-2011, 2011.

Huguet, C., De Lange, G. J., Middelburg, J. J., Sinninghe Damsté, J. S., and Schouten, S.: Selective preservation of soil organic matter in oxidized marine sediments (Madeira Abyssal Plain), Geochim. Cosmochim. Ac., 72, 6061–6068, 2008.

Iakovleva, A. I., Brinkhuis, H., and Cavagnetto, C.: Late Palaeocene-Early Eocene dinoflagellate cysts from the Turgay Strait, Kazakhstan; correlations across ancient seaways, Palaeogeogr. Palaeocl., 172, 243–268, 2001.

Ingram, S. L.: The Tuscahoma-Bashi section at Meridian, Mississippi: First notice of lowstand deposits above the Paleocene-Eocene TP2/TE1 sequence boundary, Mississippi Geol., 11, 9–14, 1991.

Joachimski, M. M., Ostertag-Henning, C., Pancost, R. D., Strauss, H., Freeman, K. H., Littke, R., Sinninghe Damsté, J. S., and Racki, G.: Water column anoxia, enhanced productivity, and concomitant changes in $\delta^{13}C$ and $\delta^{34}S$ across the Frasnian-Femennian boundary (Kowala – Holy Cross Mountains/Poland), Chem. Geol., 175, 109–131, 2001.

John, C. M., Bohaty, S. M., Zachos, J. C., Sluijs, A., Gibbs, S. J., Brinkhuis, H., and Bralower, T. J.: North American continental margin records of the Paleocene-Eocene thermal maximum: Implications for global carbon and hydrological cycling, Paleoceanography, 23, PA2217, doi:10.1029/2007PA001465, 2008.

John, C. M., Banerjee, N. R., Longstaffe, F. J., Sica, C., Law, K. R., and Zachos, J. C.: Clay assemblage and oxygen isotopic constraints on the weathering response to the Paleocene-Eocene thermal maximum, east coast of North America, Geology, 40, 591–594, doi:10.1130/g32785.1, 2012.

Jorissen, F. J., de Stigter, H. C., and Widmark, J. G. V.: A conceptual model explaining benthic foraminiferal microhabitats, Mar. Micropaleontol., 26, 3–15, 1995.

Keating-Bitonti, C. R., Ivany, L. C., Affek, H. P., Douglas, P., and Samson, S. D.: Warm, not super-hot, temperatures in the early Eocene subtropics, Geology, 39, 771–774, 2011.

Kenig, F., Hudson, J. D., Sinninghe Damsté, J. S., and Popp, B. N.: Intermittent euxinia: Reconciliation of a Jurassic black shale with its biofacies, Geology, 32, 421–424, 2004.

Kennett, J. P. and Stott, L. D.: Abrupt deep-sea warming, palaeoceanographic changes and benthic extinctions at the end of the Palaeocene, Nature, 353, 225–229, 1991.

Kim, J.-H., van der Meer, J., Schouten, S., Helmke, P., Willmott, V., Sangiorgi, F., Koç, N., Hopmans, E. C., and Sinninghe Damsté, J. S.: New indices and calibrations derived from the distribution of crenarchaeal isoprenoid tetraether lipids: Implications for past sea surface temperature reconstructions, Geochim. Cosmochim. Ac., 74, 4639–4654, 2010.

Knies, J., Mann, U., Popp, B. N., Stein, R., and Brumsack, H.-J.: Surface water productivity and paleoceanographic implications in the Cenozoic Arctic Ocean, Paleoceanography, 23, PA1S16, doi:10.1029/2007pa001455, 2008.

Kopp, R. E., Schumann, D., Raub, T. D., Powars, D. S., Godfrey, L. V., Swanson-Hysell, N. L., Maloof, A. C., and Vali, H.: An Appalachian Amazon? Magnetofossil evidence for the development of a tropical river-like system in the mid-Atlantic United States during the Paleocene-Eocene thermal maximum, Paleoceanography, 24, PA4211, doi:10.1029/2009pa001783, 2009.

Kuypers, M. M. M., van Breugel, Y., Schouten, S., Erba, E., and Damsté, J. S. S.: N_2-fixing cyanobacteria supplied nutrient N

for Cretaceous oceanic anoxic events, Geology, 32, 853–856, doi:10.1130/g20458.1, 2004.

Kuypers, M. M. M., Lavik, G., Woebken, D., Schmid, M., Fuchs, B. M., Amann, R., Jørgensen, B. B., and Jetten, M. S. M.: Massive nitrogen loss from the Benguela upwelling system through anaerobic ammonium oxidation, P. Natl. Acad. Sci. USA, 102, 6478–6483, doi:10.1073/pnas.0502088102, 2005.

Lourens, L. J., Sluijs, A., Kroon, D., Zachos, J. C., Thomas, E., Röhl, U., Bowles, J., and Raffi, I.: Astronomical pacing of late Palaeocene to early Eocene global warming events, Nature, 435, 1083–1087, 2005.

Lunt, D. J., Dunkley Jones, T., Heinemann, M., Huber, M., LeGrande, A., Winguth, A., Loptson, C., Marotzke, J., Roberts, C. D., Tindall, J., Valdes, P., and Winguth, C.: A model–data comparison for a multi-model ensemble of early Eocene atmosphere–ocean simulations: EoMIP, Clim. Past, 8, 1717–1736, doi:10.5194/cp-8-1717-2012, 2012.

Mancini, E. A.: Lithostratigraphy and biostratigraphy of Paleocene subsurface strata in southwest Alabama, T. Gulf Coast Assoc. Geol. Soc., 31, 359–367, 1981.

Mancini, E. A. and Oliver, G. E.: Planktic foraminifers from the Tuscahoma Sand (upper Paleocene) of southwest Alabama, Micropaleontology, 27, 204–225, 1981.

Mancini, E. A. and Tew, B. H.: Relationships of Paleogene stage and planktonic foraminiferal zone boundaries to lithostratigraphic and allostratigraphic contacts in the eastern Gulf Coastal Plain, J. Foramin. Res., 21, 48–66, 1991.

Mancini, E. A. and Tew, B. H.: Sequence stratigraphy of Paleogene strata of the eastern limb of the Mississippi Embayment, Guidebook for Field Trip #8 in American Association of Petroleum Geologists Annual Convention New Orleans, LA, 1993.

Mancini, E. A. and Tew, B. H.: Geochronology, biostratigraphy, and sequence stratigraphy of a marginal marine shelf stratigraphic succession: Upper Paleocene and Lower Eocene, Wilcox Group, eastern Gulf Coast plain, USA, in: Geochronology, time scales and global stratigraphic correlation, S edited by: Berggren, W. A., Kent, D. V., Aubry, M.-P., and Hardenbol, J., EPM (Society of Sedimentary Geology) Special Publication, 54, 281–293, 1995.

Markwick, P. J.: The palaeogeographic and palaeoclimatic significance of climate proxies for data-model comparisons, in: Deep-time perspectives on climate change: marrying the signal from computer models and biological proxies, edited by: M. Williams, A. M. H., Gregory, F. J., and Schmidt, D. N., The Micropalaeontological Society Special Publications. The Geological Society, London, 2007.

Martini, E.: Standard Tertiary and Quaternary calcareous nannoplankton zonation, in: Proceedings of the II Planktonic Conference, Roma 1970, Vol. 2, edited by: Farinacci, A., Edizioni Tecnoscienza, Rome, 739–785, 1971.

McInerney, F. A. and Wing, S. L.: The Paleocene-Eocene Thermal Maximum: A Perturbation of Carbon Cycle, Climate, and Biosphere with Implications for the Future, Annu. Rev. Earth Pl. Sc., 39, 489–516, 2011.

Monechi, S. and Angori, E.: Calcareous nannofossil biostratigraphy of the Paleocene/Eocene Boundary, Ocean Drilling Program Leg 208 Hole 1266C, in: Proceedings of the Ocean Drilling Program, Scientific Results 208, edited by: Kroon, D., Zachos, J. C., and Richter, C., Ocean Drilling Program, College Station, TX, 1-9, 2006.

Moss, P. T., Kershaw, A. P., and Grindrod, J.: Pollen transport and deposition in riverine and marine environments within the humid tropics of northeastern Australia, Rev. Palaeobot. Palyno., 134, 55–69, doi:10.1016/j.revpalbo.2004.11.003, 2005.

Murphy, B. H., Farley, K. A., and Zachos, J. C.: An extraterrestrial 3He-based timescale for the Paleocene-Eocene thermal maximum (PETM) from Walvis Ridge, IODP Site 1266, Geochim. Cosmochim. Ac., 74, 5098–5108, 2010.

Mutterlose, J., Linnert, C., and Norris, R.: Calcareous nannofossils from the Paleocene-Eocene Thermal Maximum of the equatorial Atlantic (ODP Site 1260B): Evidence for tropical warming, Mar. Micropaleontol., 65, 13–31, 2007.

Nicolo, M. J., Dickens, G. R., and Hollis, C. J.: South Pacific intermediate water oxygen depletion at the onset of the Paleocene-Eocene Thermal Maximum as depicted in New Zealand margin sections, Paleoceanography, 25, PA4210, doi:10.1029/2009PA001904, 2010.

Pälike, C., Delaney, M. L., and Zachos, J. C.: Deep sea redox across the Paleocene-Eocene thermal maximum, Geochem. Geophy. Geosy., 15, 1038–1053, doi:10.1002/2013GC005074, 2014.

Pardo, A., Keller, G., Molina, E., and Canudo, J.: Planktic foraminiferal turnover across the Paleocene-Eocene transition at DSDP Site 401, Bay of Biscay, North Atlantic, Mar. Micropaleontol., 29, 129–158, 1997.

Paytan, A., Averyt, K., Faul, K., Gray, E., and Thomas, E.: Barite accumulation, ocean productivity, and Sr/Ba in barite across the Paleocene-Eocene Thermal Maximum, Geology, 35, 1139–1142, 2007.

Perch-Nielsen, K.: Cenozoic calcareous nannofossils, in: Plankton Stratigraphy, edited by: Bolli, H. M., Saunders, J. B., and Perch-Nielsen, K., Cambridge university Press, 427–554, 1985.

Peterse, F., Kim, J.-H., Schouten, S., Kristensen, D. K., Koç, N., and Sinninghe Damsté, J. S.: Constraints on the application of the MBT/CBT palaeothermometer at high latitude environments (Svalbard, Norway), Org. Geochem., 40, 692–699, 2009.

Peterse, F., van der Meer, J., Schouten, S., Weijers, J. W. H., Fierer, N., Jackson, R. B., Kim, J. H., and Sinninghe Damsté, J. S.: Revised calibration of the MBT/CBT paleotemperature proxy based on branched tetraether membrane lipids in surface soils, Geochim. Cosmochim. Ac., 96, 215–229, 2012.

Prothero, D. R. and Schwab, F.: Sedimentary Geology (2nd Edition), Freeman and Company, New York, 2004.

Rhodes, G. M., Ali, J. R., Hailwood, E. A., King, C., and Gibson, T. G.: Magnetostratigraphic correlation of Paleogene sequences from northwest Europe and North America, Geology, 28, 927–930, 1999.

Ridgwell, A. and Schmidt, D. N.: Past constraints on the vulnerability of marine calcifiers to massive carbon dioxide release, Nature Geosci, 3, 196–200, 2010.

Röhl, U., Westerhold, T., Bralower, T. J., and Zachos, J. C.: On the duration of the Paleocene – Eocene thermal maximum (PETM), Geochem. Geophy. Geosy., 8, Q12002, doi:10.1029/2007GC001784, 2007.

Schoon, P. L., Sluijs, A., Sinninghe Damsté, J. S., and Schouten, S.: High productivity and elevated carbon isotope fractionations in the Arctic Ocean during Eocene Thermal Maximum 2, Paleoceanography, 26, PA3215, doi:10.1029/2010PA002028, 2011.

Schouten, S., Huguet, C., Hopmans, E. C., Kienhuis, M. V. M., and Sinninghe Damsté, J. S.: Analytical Methodology for TEX_{86}

Paleothermometry by High-Performance Liquid Chromatography/Atmospheric Pressure Chemical Ionization-Mass Spectrometry, Anal. Chem., 79, 2940–2944, 2007.

Sessa, J. A., Bralower, T. J., Patzkowsky, M. E., Handley, J. C., and Ivany, L. C.: Environmental and biological controls on the diversification and ecological reorganization of Late Cretaceous and early Paleogene marine ecosystems in the Gulf Coastal Plain, Paleobiology, 38, 218–239, 2012a.

Sessa, J. A., Ivany, L. C., Schlossnagle, T. H., Samson, S. D., and Schellenberg, S. A.: The fidelity of oxygen and strontium isotope values from shallow shelf settings: Implications for temperature and age reconstructions, Palaeogeography, Palaeoclimatology, Palaeoecology, 342–343, 27–39, 2012b.

Siesser, W. G.: Paleogene calcareous nannoplankton biostratigraphy: Mississippi, Alabama and Tennessee, Mississippi Department of Natural Resources Bureau of Geology Bulletin, 125, 1–61, 1983.

Sinninghe Damsté, J. S. and Hopmans, E. C.: Does fossil pigment and DNA data from Mediterranean sediments invalidate the use of green sulfur bacterial pigments and their diagenetic derivatives as proxies for the assessment of past photic zone euxinia?, Environ. Microbiol., 10, 1392–1399, doi:10.1111/j.1462-2920.2008.01609.x, 2008.

Sinninghe Damsté, J. S. and Köster, J.: A euxinic southern North Atlantic Ocean during the Cenomanian/Turonian oceanic anoxic event, Earth Planet. Sci. Lett., 158, 165–173, 1998.

Sinninghe Damsté, J. S., Rijpstra, W. I. C., Leeuw, J. W. d., and Schenk, P. A.: Origin of organic sulphur compounds and sulphur-containing high molecular weight substances in sediments and immature crude oils, Org. Geochem., 13, 593–606, 1988.

Sinninghe Damsté, J. S., Wakeham, S. G., Kohnen, M. E. L., Hayes, J. M., and de Leeuw, J. W.: A 6,000-year sedimentary molecular record of chemocline excursions in the Black Sea, Nature, 362, 827–829, 1993.

Slomp, C. P. and Van Cappellen, P.: The global marine phosphorus cycle: sensitivity to oceanic circulation, Biogeosciences, 4, 155–171, doi:10.5194/bg-4-155-2007, 2007.

Sluijs, A. and Brinkhuis, H.: A dynamic climate and ecosystem state during the Paleocene-Eocene Thermal Maximum: inferences from dinoflagellate cyst assemblages on the New Jersey Shelf, Biogeosciences, 6, 1755–1781, doi:10.5194/bg-6-1755-2009, 2009.

Sluijs, A. and Dickens, G. R.: Assessing offsets between the δ^{13}C of sedimentary components and the global exogenic carbon pool across Early Paleogene carbon cycle perturbations, Global Biogeochem. Cy., 26, GB4005, doi:10.1029/2011GB004224, 2012.

Sluijs, A., Schouten, S., Pagani, M., Woltering, M., Brinkhuis, H., Sinninghe Damsté, J. S., Dickens, G. R., Huber, M., Reichart, G.-J., Stein, R., Matthiessen, J., Lourens, L. J., Pedentchouk, N., Backman, J., Moran, K., and the Expedition 302 Scientists: Subtropical Arctic Ocean temperatures during the Palaeocene/Eocene thermal maximum, Nature, 441, 610–613, 2006.

Sluijs, A., Bowen, G. J., Brinkhuis, H., Lourens, L. J., and Thomas, E.: The Palaeocene-Eocene thermal maximum super greenhouse: biotic and geochemical signatures, age models and mechanisms of global change, in: Deep time perspectives on Climate Change: Marrying the Signal from Computer Models and Biological Proxies, edited by: Williams, M., Haywood, A. M., Gregory, F. J., and Schmidt, D. N., The Micropalaeontological Society, Special Publications. The Geological Society, London, London, 323–347, 2007a.

Sluijs, A., Brinkhuis, H., Schouten, S., Bohaty, S. M., John, C. M., Zachos, J. C., Reichart, G.-J., Sinninghe Damsté, J. S., Crouch, E. M., and Dickens, G. R.: Environmental precursors to light carbon input at the Paleocene/Eocene boundary, Nature, 450, 1218–1221, 2007b.

Sluijs, A., Brinkhuis, H., Crouch, E. M., John, C. M., Handley, L., Munsterman, D., Bohaty, S., M., Zachos, J. C., Reichart, G.-J., Schouten, S., Pancost, R. D., Sinninghe Damsté, J. S., Welters, N. L. D., Lotter, A. F., and Dickens, G. R.: Eustatic variations during the Paleocene-Eocene greenhouse world, Paleoceanography, 23, PA4216, doi:10.1029/2008PA001615, 2008a.

Sluijs, A., Röhl, U., Schouten, S., Brumsack, H.-J., Sangiorgi, F., Sinninghe Damsté, J. S., and Brinkhuis, H.: Arctic late Paleocene–early Eocene paleoenvironments with special emphasis on the Paleocene-Eocene thermal maximum (Lomonosov Ridge, Integrated Ocean Drilling Program Expedition 302), Paleoceanography, 23, PA1S11, doi:10.1029/2007PA001495, 2008b.

Sluijs, A., Schouten, S., Donders, T. H., Schoon, P. L., Röhl, U., Reichart, G. J., Sangiorgi, F., Kim, J.-H., Sinninghe Damsté, J. S., and Brinkhuis, H.: Warm and Wet Conditions in the Arctic Region during Eocene Thermal Maximum 2, Nat. Geosci., 2, 777–780, 2009.

Sluijs, A., Bijl, P. K., Schouten, S., Röhl, U., Reichart, G.-J., and Brinkhuis, H.: Southern ocean warming, sea level and hydrological change during the Paleocene-Eocene thermal maximum, Clim. Past, 7, 47–61, doi:10.5194/cp-7-47-2011, 2011.

Smith, T., Rose, K., D., and Gingerich, P., D.: Rapid Asia–Europe–North America geographic dispersal of earliest Eocene primate *Teilhardina* during the Paleocene–Eocene Thermal Maximum, P. Natl. Acad. Sci. USA, 103, 11223–11227, 2006.

Sømme, T. O., Helland-Hansen, W., and Granjeon, D.: Impact of eustatic amplitude variations on shelf morphology, sediment dispersal, and sequence stratigraphic interpretation: Icehouse versus greenhouse systems, Geology, 37, 587–590, 2009.

Speijer, R. P. and Morsi, A.-M. M.: Ostracode turnover and sea-level changes associated with the Paleocene-Eocene thermal maximum, Geology, 30, 23–26, 2002.

Speijer, R. P. and Wagner, T.: Sea-level changes and black shales associated with the late Paleocene thermal maximum: Organic-geochemical and micropaleontologic evidence from the southern Tethyan margin (Egypt-Israel), Geol. Soc. Am. SP, 356, 533–549, 2002.

Taylor, K. W. R., Huber, M., Hollis, C. J., Hernandez-Sanchez, M. T., and Pancost, R. D.: Re-evaluating modern and Palaeogene GDGT distributions: Implications for SST reconstructions, Global Planet. Change, 108, 158–174, doi:10.1016/j.gloplacha.2013.06.011, 2013.

Thomas, E.: Cenozoic mass extinctions in the deep sea: what perturbs the largest habitat on earth?, in: Geological Society of America Special Paper 424, edited by: Monechi, S., Coccioni, R., and Rampino, M., Geological Society of America, Bolder, Colorado, 1–24, 2007.

Thomas, E. and Shackleton, N. J.: The Palaeocene-Eocene benthic foraminiferal extinction and stable isotope anomalies., in: Correlation of the Early Paleogene in Northwestern Europe, Geological Society London Special Publication, 101, edited by: Knox, R.

W. O. B., Corfield, R. M., and Dunay, R. E., Geological Society of London, London, United Kingdom, 401–441, 1996.

Thomas, E. and Zachos, J. C.: Was the late Paleocene thermal maximum a unique event?, Geologiska Föreningens i Stockholm Förhandlingar (GFF; Transactions of the Geological Society in Stockholm), 122, 169–170, 2000.

Thrasher, B. L. and Sloan, L. C.: Carbon dioxide and the early Eocene climate of western North America, Geology, 37, 807–810, 2009.

Tripati, A. and Elderfield, H.: Deep-Sea Temperature and Circulation Changes at the Paleocene-Eocene Thermal Maximum, Science, 308, 1894–1898, 2005.

Tsandev, I. and Slomp, C. P.: Modeling phosphorus cycling and carbon burial during Cretaceous Oceanic Anoxic Events, Earth Planet. Sci. Lett., 286, 71–79, 2009.

Tschudy, R. H.: Stratigraphic distribution of significant Eocene palynomorphs of the Mississippi Embayment, US Geological Survey Professional Paper 743-B, US Geological Survey, United States Government Printing Office, Washington, 1973.

Tyrrell, T.: The relative influences of nitrogen and phosphorus on oceanic primary production, Nature, 400, 525–531, 1999.

Vandenberghe, N., Speijer, R. P., and Hilgen, F. J.: The Paleogene Period, in: The Geologic Time Scale 2012, edited by: Gradstein, F. M., Ogg, J. G., Schmitz, M., and Ogg, G., Elsevier, 855–921, 2012.

Volkman, J. K.: A review of sterol markers for marine and terrigenous organic matter, Org. Geochem., 9, 83–99, 1986.

Wade, B. S., Pearson, P. N., Berggren, W. A., and Pälike, H.: Review and revision of Cenozoic tropical planktonic foraminiferal biostratigraphy and calibration to the geomagnetic polarity and astronomical time scale, Earth-Sci. Rev., 104, 111–142, doi:10.1016/j.earscirev.2010.09.003, 2011.

Weijers, J. W. H., Schouten, S., Spaargaren, O. C., and Sinninghe Damsté, J. S.: Occurrence and distribution of tetraether membrane lipids in soils: Implications for the use of the TEX_{86} proxy and the BIT index, Org. Geochem., 37, 1680–1693, 2006.

Weijers, J. W. H., Schouten, S., van den Donker, J. C., Hopmans, E. C., and Sinninghe Damste, J. S.: Environmental controls on bacterial tetraether membrane lipid distribution in soils, Geochim. Cosmochim. Ac., 71, 703–713, 2007.

Wing, S. L. and Currano, E. D.: Plant response to a global greenhouse event 56 million years ago„ Am. J. Bot., 100, 1234–1254, 2013.

Wing, S. L., Harrington, G. J., Smith, F. A., Bloch, J. I., Boyer, D. M., and Freeman, K. H.: Transient Floral Change and Rapid Global Warming at the Paleocene-Eocene Boundary, Science, 310, 993–996, doi:10.1126/science.1116913, 2005.

Winguth, A. M. E., Thomas, E., and Winguth, C.: Global decline in ocean ventilation, oxygenation, and productivity during the Paleocene-Eocene Thermal Maximum: Implications for the benthic extinction, Geology, 40, 263–266, doi:10.1130/g32529.1, 2012.

Wolfe, J. A. and Dilcher, D. L.: Late Paleocene through Middle Eocene climates in lowland North America, Geologiska Föreningens i Stockholm Förhandlingar (GFF; Transactions of the Geological Society in Stockholm), 122, 184–185, 2000.

Yao, W. and Millero, F. J.: The Chemistry of the Anoxic Waters in the Framvaren Fjord, Norway, Aquat. Geochem., 1, 53–88, 1995.

Zachos, J. C., Wara, M. W., Bohaty, S., Delaney, M. L., Petrizzo, M. R., Brill, A., Bralower, T. J., and Premoli Silva, I.: A transient rise in tropical sea surface temperature during the Paleocene-Eocene thermal maximum, Science, 302, 1551–1554, 2003.

Zachos, J. C., Schouten, S., Bohaty, S., Quattlebaum, T., Sluijs, A., Brinkhuis, H., Gibbs, S., and Bralower, T. J.: Extreme warming of mid-latitude coastal ocean during the Paleocene-Eocene Thermal Maximum: Inferences from TEX_{86} and Isotope Data, Geology, 34, 737–740, 2006.

Zachos, J. C., Dickens, G. R., and Zeebe, R. E.: An early Cenozoic perspective on greenhouse warming and carbon-cycle dynamics, Nature, 451, 279–283, 2008.

Zeebe, R. E., Zachos, J. C., and Dickens, G. R.: Carbon dioxide forcing alone insufficient to explain Palaeocene-Eocene Thermal Maximum warming, Nat. Geosci., 2, 576–580, 2009.

Zonneveld, K. A. F., Marret, F., Versteegh, G. J. M., Bogus, K., Bonnet, S., Bouimetarhan, I., Crouch, E., de Vernal, A., Elshanawany, R., Edwards, L., Esper, O., Forke, S., Grvøsfjeld, K., Henry, M., Holzwarth, U., Kielt, J.-F. ß., Kim, S.-Y., Ladouceur, S. p., Ledu, D., Chen, L., Limoges, A., Londeix, L., Lu, S. H., Mahmoud, M. S., Marino, G., Matsouka, K., Matthiessen, J., Mildenhal, D. C., Mudie, P., Neil, H. L., Pospelova, V., Qi, Y., Radi, T., Richerol, T., Rochon, A., Sangiorgi, F., Solignac, S., Turon, J.-L., Verleye, T., Wang, Y., Wang, Z., and Young, M.: Atlas of modern dinoflagellate cyst distribution based on 2405 data points, Rev. Palaeobot. Palynol., 191, 1–197, doi:10.1016/j.revpalbo.2012.08.003, 2013.